NUMERICAL STUDY OF THE EFFECTS OF RADIATION ON NATURAL CONVECTION FLOW FROM A POROUS VERTICAL PLATE IN PRESENCE OF HEAT GENERATION

Submitted by
AMENA FERDOUSI
Student No. 100509004P
Session: October-2005

MASTER OF PHILOSOPHY
IN
MATHEMATICS

Department of Mathematics
BANGLADESH UNIVERSITY OF ENGINEERING AND TECHNOLOGY, DHAKA-1000
April - 2009

The thesis entitled

NUMERICAL STUDY OF THE EFFECTS OF RADIATION ON NATURAL CONVECTION FLOW FROM A POROUS VERTICAL PLATE IN PRESENCE OF HEAT GENERATION

Submitted by

AMENA FERDOUSI

Student No. 100509004P, Session: October-2005, a part time student of M. Phil. (Mathematics) has been accepted as satisfactory in partial fulfillment for the degree of

Master of Philosophy in Mathematics

on April, 04 - 2009

BOARD OF EXAMINERS

1 A. Alim 04/04/09

Dr. Md. Abdul Alim — Chairman (Supervisor)
Associate Professor
Dept. of Mathematics, BUET, Dhaka-1000

2 4.4.09

Head — Member (Ex-Officio)
Dept. of Mathematics
BUET, Dhaka-1000

3 4.4.09

Dr. Md. Mustafa Kamal Chowdhury — Member
Professor
Dept. of Mathematics, BUET, Dhaka-1000

4. Selina Parvin 4.04.2009

Dr. Selina Parvin — Member (External)
Professor
Dept. of Mathematics, Dhaka University, Dhaka-1000

Abstract

In this thesis, the effects of radiation on magnetohydrodynamic(MHD) natural convection flow from a porous vertical plate in presence of heat generation has been scrutinized. A set of different governing equations along with the corresponding boundary conditions of the physical problems are represented mathematically. Finite-difference methods accompanied by the Keller box scheme are used for the numerical solution of the governing equations that contain the equations of continuity, momentum and energy equations are altered into a set of non-dimensional boundary layer equations in conjunction with the corresponding boundary conditions by using the appropriate transformation. All through the concentration is paid on the assessment of the surface shear stress in terms of local skin friction, rate of heat transfer in terms of local Nusselt number, velocity profiles in addition to temperature profiles. FORTRAN 90 is used to simulate the formulation of the job and to get the graphical output of the numerical values TECPLOT has been used. A collection of parameters set is also taking into account for computation consisting of heat generation parameter Q, radiation parameter R_d, surface temperature parameter θ_w, Prandtl number Pr and magnetic parameter M. The results in terms of local skin friction, local Nusselt number will be shown in tabular forms. Velocity profiles, temperature profiles, skin friction coefficient and rate of heat transfer have been exhibited graphically for various values of heat generation parameter, radiation parameter and surface temperature parameter separately and the Prandtl number as well.

Author's Declaration

I am hereby declaring that the work in this dissertation entitled "NUMERICAL STUDY OF THE EFFECTS OF RADIATION ON NATURAL CONVECTION FLOW FROM A POROUS VERTICAL PLATE IN PRESENCE OF HEAT GENERATION" is being carried out in accordance with the regulations of Bangladesh University of Engineering and Technology (BUET), Dhaka, Bangladesh .The work is also original except where indicated by and attached with special reference in the context and no part of it has been submitted for any attempt to get other degrees or diplomas.

All views expressed in the dissertation are those of the author and in no way or by no means represent those of Bangladesh University of Engineering and Technology, Dhaka. This dissertation has not been submitted to any other University for examination either in home or abroad.

Amena Ferdousi

(Amena Ferdousi)

Date: 4th April, 2009

Acknowledgements

At the outset I am pronouncing my thankfulness to the almighty who give me the ability to carry out such a research work.

My gratitude will always be there to Dr. Md. Abdul Alim, Associate Professor, Department of Mathematics, BUET, my supervisor who continuously guided me from all the directions. It is my great gratification having the opportunity to work under supervision. I would like to have the opportunity to express my heart-rending admiration to my supervisor who has encouraged and rightly initiated me to step into the wide arena of mathematics and its application in the engineering fields.

I am not less grateful and thankful to the efforts, perseverance, sincerity, enormous will-force, clarity, accuracy, completeness, monumental patience, generous co-operation and fellow-feeling he made for me to venture this research and bring this painstaking task to a successful end.

I am as well intensely beholden to all my teachers of the Department of Mathematics, BUET for their intelligent and open-minded support in providing me all necessary help from the department during my course of M. Phil. degree They all have helped me immensely over the last school period either in the course or mentally with advices

I would like to utter here the name of my colleagues of Eastern University fort their co-operation.

I am really grateful to my husband for his burly bona fide aid.

I must acknowledge my debt to my parents for whom I have been able to see the beautiful sights and sounds of the world.

Contents

Nomenclature

a_r	Rosseland mean absorption co-efficient
C_f	Local skin friction coefficient
C_p	Specific heat at constant pressure
f	Dimensionless stream function
f'	Derivative of f with respect to η
Gr	Grashof number
g	Acceleration due to gravity
k	Thermal conductivity
M	Magnetic parameter
Nu	Local Nusselt number
Pr	Prandtl number
Q	Heat generation parameter
q_r	Radiation heat flux
q_w	Heat flux at the surface
q_c	Conduction heat flux
R_d	Radiation parameter
T	Temperature of the fluid in the boundary layer
T_∞	Temperature of the ambient fluid
T_w	Temperature at the surface
(u, v)	Dimensionless velocity components along the (x, y) axes
(x, y)	Axis in the direction along and normal to the surface respectively

Greek symbols

β	Coefficient of thermal expansion
β_0	Strength of magnetic field
θ	Dimensionless temperature function
θ_w	Surface temperature parameter
μ	Viscosity of the fluid
ν	Kinematic viscosity
ρ	Density of the fluid
σ	Stephman-Boltzman constant.
σ_s	Scattering co-efficient
σ_0	Electrical conduction
τ_w	Shearing stress
ψ	Non-dimensional stream function
(ξ, η)	Dimensionless velocity components along the (x, y)axes

List of Tables

List of Figures

Chapter 1

1.1 Introduction

The effect of radiation on free convection has been drawn forth not only for its fundamental aspects but also for its significance in the contexts of space technology and processes involving high temperature. Like conduction or convection thermal radiation is not an available heat transfer process. So information on thermal radiation like thermal radiation on free convection from a vertical porous plate with heat generation will signify significant significance.

As said by Maxwell's classical electromagnetic theory, radiant energy travels in the form of electromagnetic waves and according to Planck's it travels in the form of discrete photon. The implications of electromagnetic are of interest in engineering applications. Without interacting with a medium thermal radiation is transferred. Moving over a long distance makes it of great magnitude in vacuum and space application. Thermal radiation is important during atmospheric re entry of space vehicles, in combustion applications (fires, furnace, rocket nozzles, engines etc.), in nuclear reactions (such as in the sun, in a fusion reactor or in nuclear bombs). [30]

Generally, the density difference gives rise to buoyancy forces, which drive the flow. Buoyancy induced convective flow is of great importance in many heat removal processes in engineering technology and has attracted the attention of many researchers in the last few decades due to the fact that both science and technology are being interested in passive energy storage systems, such as the cooling of spent fuel rods in nuclear power applications and the design of solar collectors. In particular, it has been ascertained that free convection induced the thermal stress, which leads to critical structural damage in the piping systems of nuclear reactors. The buoyant flow arising from heat rejection to the atmosphere, heating of rooms, fires, and many other heat transfers processes, both natural and artificial, are other examples of natural convection flows.

Porous plates is termed by the plate possess with very fine holes distributed uniformly over the entire surface of the plate through which fluid can flow freely.

The plate from which the fluid enters into the flow region is known as plate with injection and the plate from which the fluid leaves from the flow region is known as plate with

suction. Sometimes it is being necessary to controls the boundary layer flows by injecting or withdrawing a fluid through a heated boundary layer wall to enhance heating or cooling of the system. This technique is used in air craft wings. For the present problem we will consider the suction.

Magnetohydrodynamic (MHD) is the science, which deals with the motion of a highly conducting fluid in presence of a magnetic field **Error! Reference source not found.** The motion of the conducting fluid across the magnetic field generates electric currents which change the magnetic field and the action of the magnetic field on these currents give rise to mechanical forces, which modify the fluid. It is possible to attain equilibrium in a conducting fluid if the current is parallel to the magnetic field. For then, the magnetic forces vanish and the equilibrium of the gas is the same as in the absence of magnetic fields are considered force free. But most liquids and gases are poor conductors of electricity In the case when the conductor is either a liquid or a gas, electromagnetic forces will be generated which may be of the same order of magnitude as the hydrodynamical and inertial forces. Thus the equations of motion as well as the other forces will have to take these electromagnetic forces into account. The MHD was originally applied to astrophysical and geophysical problems, where it is still very important but more recently to the problem of fusion power where the application is the creation and containment of hot plasmas by electromagnetic forces, since material walls would be destroyed. Astrophysical problems include solar structure, especially in the outer layers, the solar wind bathing the earth and other planets, and interstellar magnetic fields. The primary geophysical problem is planetary magnetism, produced by currents deep in the planet, a problem that has not been solved to any degree of satisfaction.

In the absence of work done, a change in internal energy per unit volume in the material. is proportional to the change in temperature which is known as heat generation [33] The study of heat generation in moving fluids is important in view of several physical problems such as those dealing with chemical reactions and those concerned with dissociating fluids. Possible heat generation effects may alter the temperature distribution and, therefore, the particle deposition rate. This may occur in such applications related to nuclear reactor cores, fire and combustion modeling, electronic chips and semiconductor wafers. In fact, the literature is replete with examples dealing with the heat transfer in laminar flow of viscous fluids. Vajravelu and Hadjinicolaou [31] studird the heat transfer in a viscous fluid over a stretching sheet with viscous dissipation and internal heat

generation In this study, they considered that the volumetric rate of heat generation, $q'''[W/m^3]$ should be

$$q''' = \begin{cases} Q_0(T - T_\infty) & for\ T \geq T_\infty \\ 0 & for\ T < T_\infty \end{cases}$$

where Q_0 is the heat generation constant.

The above relation explained is valid as an approximation of the state of some exothermic process and having T_∞ as the onset temperature. When the inlet temperature is not less than T_∞ they used $Q_0(T- T_\infty)$. To our best knowledge, the heat generation effect on MHD free convection flow on a porous plate with constant heat flux has not been studied yet, and the present work demonstrates the issue

The cases of incompressible viscous fluid such as continuity equation, momentum equation and energy equation are deal with the governing partial differential equations and the radiation energy emitted by a body is transmitted in the space in the form of electromagnetic waves.

Merkin [5] studied free convection with blowing and suction. Lin and Yu [16] studied free convection on a horizontal plate with blowing and suction. Hossain, et al. [1] studied the effect of radiation on free convection flow from a porous vertical plate. Soundalgekar et al [2] studied the combined free and forced convection flow past a semi infinite vertical plate with variable surface temperature. Hossain and Takhar [3] studied radiation effect on mixed convection along a vertical plate with uniform surface temperature. Sparrow and Cess [4] studied free convection with blowing or suction. Molla et al. [6] studied natural convection flow along a vertical wavy surface with uniform surface temperature in presence of heat generation/absorption. Ali [7] studied the effect of radiation on free convection flows on sphere with heat generation. Akhter [8] studied the effect of radiations on free convection flow on sphere with isothermal surface and uniform heat flux. None of the aforementioned studies, considered the heat generation effects on laminar boundary layer flow of the fluids along porous plate with radiation heat loss. Cogley et al.[9] studied differential approximation for radiative in a non-gray gas near equilibrium. Eichhorn [10] studied the effect of mass transfer on free convection. Clarke [11] studied Transpiration and natural convection on the vertical flat plate problem. . Merkin [12] studied the effects of blowing and suction on free convection boundary layers. Vedhanayagam et al. [13] a transformation of the boundary layer equations for free

convection past a vertical flat plate with arbitrary blowing and wall temperature variations Clarke and Riley [14] studied natural convection induced in a gas by the presence of a hot porous horizontal surface. Clarke and Riley [15] studied free convection and the burning of a horizontal fuel surface. Keller [17] applied numerical methods in boundary layer theory. Ali et al. [18] studied natural convection- radiation interaction in boundary layer flow over horizontal surfaces. Siegel and Howell [19] studied thermal Radiation Heat Transfer. Sparrow and Yu [20] studied local non similarity thermal boundary layer solutions. Chen [21] studied parabolic systems on local non-similarity method. Hossain et al. [22] studied non-darcy forced convection boundary layer flow over a wedge embedded in a saturated porous medium. Cebeci and Bradshaw [23] studied physical and computational aspects of convective heat transfer. Hossain [24] studied effect of transpiration on combined heat and mass transfer in mixed convection along a vertical plate. Butcher [25] studied implicit Runge-Kutta processes. Nachtsheim and Swigert [26] studied satisfaction of asymptotic boundary conditions in numerical solution of systems of non-linear equation of boundary layer type. Na [27] studied computational method in engineering boundary value problems. Ozisik [28] studied radiative transfer and interactions with conduction and convection. Molla et al. [29] studied Magnetohydrodynamic natural convection flow on a sphere with uniform heat flux in presence of heat generation.

Many researchers have studied the Problems of free convection boundary layer flow over or on a various types of shapes.

In the present work, the effects of radiation on free convection flow from a porous plate in presence of heat generation have been investigated. The results will be obtained for different values of relevant physical parameters We have considered the natural convection boundary layer flow from a porous plate of an electrically conducting and steady viscous incompressible fluid in presence of strong magnetic field and heat generation with constant heat flux.

The governing partial differential equations are reduced to locally non-similar partial differential forms by adopting some appropriate transformations. The transformed boundary layer equations are solved numerically using implicit finite difference scheme with the Keller box technique [17]. The results in terms of local skin friction, local nusselt number will be shown in tabular forms. Surface shear stress in terms of local skin friction and the rate of heat transfer in terms of local Nusselt number, velocity profiles as well as

temperature profiles have been displayed graphically for selected values of parameters consisting of heat generation parameter Q, the magnetic parameter M Prandtl number Pr and the radiation parameter R_d.

In chapter 2, we have investigated the effect of radiation on natural convection flow from a porous plate in presence of heat generation. The non-dimensional boundary layer equations are solved by using implicit finite difference methods [23]. The results in terms of local skin friction, local Nusselt number will be shown in tabular forms. Velocity profiles, temperature profiles, skin friction coefficient and heat transfer coefficient will be displayed graphically for the wide range of heat generation parameter, radiation parameter and surface temperature parameter separately while the Prandtl number is to be taken 0.8 to 1.15 likely

In chapter-3, we have investigated the effect of radiation on magnetohydrodynamic natural convection flow from a porous plate in presence of heat generation. Numerical results have been shown in terms of local skin friction, the rate of heat transfer, velocity profiles as well as temperature profiles for a selection of relevant physical parameters set.

Chapter 2

Effect of Radiation on Natural Convection Flow from a Porous Vertical Plate in Presence of Heat Generation

2.1 Introduction

The effect of radiation on natural convection flow from a porous vertical plate in presence of heat generation is portrayed in this chapter. In the presence of radiation, the effects of the natural convection laminar flow from a porous vertical plate immersed in a viscous incompressible optically thin fluid have been scrutinized. The governing boundary layer equations are first transformed into a non-dimensional form and the resulting nonlinear system of partial differential equations are then solved numerically using a very efficient finite-difference method known as the Keller-box scheme. Over the work the attention is confered on the evolution of the shear stress in terms of local skin friction and the rate of heat transfer in terms of local Nusselt number, velocity profiles as well as temperature profiles for some selected values of parameters set consisting of heat generation parameter Q, radiation parameter R_d, surface temperature parameter θ_w and the Prandlt number Pr.

2.2 Formulation of the problem:

In the presence of heat generation, natural convection boundary layer flow from a porous vertical plate of a steady two dimensional viscous incompressible fluid and the radiated heat transfer has been investigated. Over the work it is assumed that the surface temperature of the porous vertical plate, T_w, is constant, where $T_w > T_\infty$. Here T_∞ is the ambient temperature of the fluid, T is the temperature of the fluid in the boundary layer. g is the acceleration due to gravity, the fluid is assumed to be a grey emitting and absorbing, but non scattering medium. In the present work following assumptions are made:

i) Variations in fluid properties are limited only to those density variations which affect the buoyancy terms

ii) Viscous dissipation effects are negligible and

iii) The radiative heat flux in the x-direction is considered negligible in comparison with that in the y direction, where the physical coordinates (u, v) are velocity components along the (x, y) axes. The physical configuration considered is as shown in Fig.2.1:

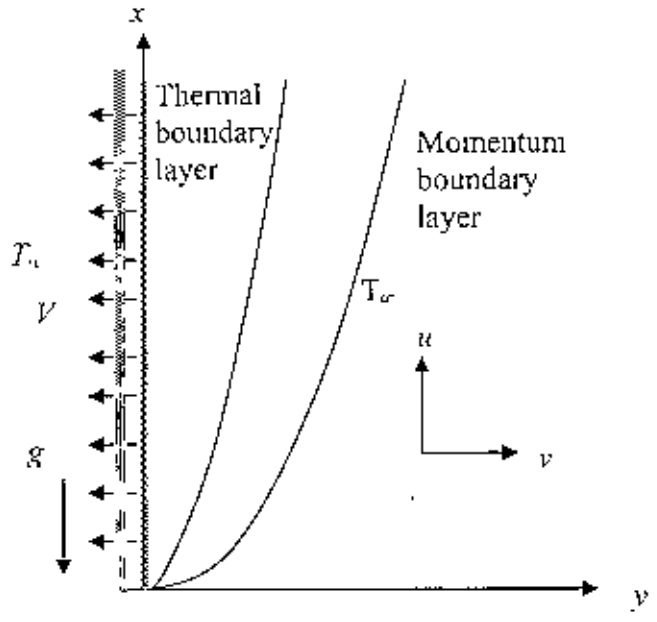

Figure: 2.1 The coordinate system and the physical model

The conservation equations for the flow characterized with steady, laminar and two dimensional boundary layer; under the usual Boussinesq approximation, the continuity, momentum and energy equation can be written as:

$$\frac{\partial u}{\partial x}+\frac{\partial v}{\partial y}=0 \tag{2.1}$$

$$\rho\left(u\frac{\partial u}{\partial x}+v\frac{\partial u}{\partial y}\right)=\mu\frac{\partial^2 u}{\partial x^2}+\rho g\beta(T-T_\infty) \tag{2.2}$$

$$\rho c_p\left(u\frac{\partial T}{\partial x}+v\frac{\partial T}{\partial y}\right)=k\frac{\partial^2 T}{\partial y^2}-\frac{\partial q_r}{\partial y}+Q_0(T-T_\infty) \tag{2.3}$$

With the boundary conditions

$$\begin{aligned} &x=0, y>0, u=0, T=T_\infty, \\ &y=0, x>0, u=0, v=V, T=T_w \\ &y\to\infty, x>0, u=0, T=T_\infty \end{aligned} \tag{2.4}$$

where ρ is the density, k is the thermal conductivity, β is the coefficient of thermal expansion, ν is the reference kinematic viscosity $\nu = \mu/\rho$, μ is the viscosity of the fluid,

C_p is the specific heat due to constant pressure and q_r is the radiative heat flux in the y direction. In order to reduce the complexity of the problem and to provide a means of comparison with future studies that will employ a more detail representation for the radiative heat flux; we will consider the optically thick radiation limit. Thus radiation heat flux term is simplified by the Rosseland diffusion approximation [Özisik (1973)] and is given by

$$q_r = -\frac{4\sigma}{3(a_r + \sigma_s)}\frac{\partial T^4}{\partial y} \tag{2.5}$$

In Equation (2.5) a_r is the Rosseland mean absorption co-efficient, σ_s is the scattering co-efficient and σ is the Stephan-Boltzman constant.

Now introduce the following non-dimensional variables:

$$\eta = \frac{y}{\xi} \tag{2.6}$$

$$\xi = \nu\left\{\frac{4x}{\nu^2 g\beta\Delta T}\right\}^{\frac{1}{4}} \tag{2.7}$$

$$\psi = \nu^{-1}\nu^2 g\beta\Delta T\xi^3\left\{f + \frac{\xi}{4}\right\}$$

$$\theta = \frac{T - T_\infty}{T_w - T_\infty} \tag{2.8}$$

$$\theta_w = \frac{T_w}{T_\infty},\quad \Delta = \theta_w - 1 = \frac{T_w}{T_\infty} - 1 = \frac{T_w - T_\infty}{T_\infty},\quad Rd = \frac{4\sigma T_\infty^3}{k(a+\sigma_s)}$$

Where, θ is the non-dimensional temperature function, θ_w is the surface temperature parameter and R_d is the radiation parameter.

Substituting (2.8) into Equations (2.1), (2.2) and (2.3) leads to the following non-dimensional equations

$$f''' + \theta - 2f'^2 + 3ff'' + \xi f'' = \xi\left(f'\frac{\partial f'}{\partial \xi} - f''\frac{\partial f'}{\partial \xi}\right) \tag{2.9}$$

$$\frac{1}{pr}\frac{\partial}{\partial \eta}\left[\left\{1 + \frac{4}{3}Rd\left(1 + (\theta_w - 1)\theta\right)^3\right\}\frac{\partial \theta}{\partial \eta}\right] + Q\theta\xi^2 + 3f\theta' + \xi\theta' = \xi\left(f'\frac{\partial \theta}{\partial \xi} - \frac{\partial f}{\partial \xi}\theta'\right) \tag{2.10}$$

Where $Pr=\mu C_p/k$ is the Prandtl number and $Q=\nu Q_0\xi^2/\nu^2\rho C_p$ is the heat generation parameter.

The boundary conditions (2.4) become

$$\begin{aligned} &f=0, f'=0, \theta=1 \text{ at } \eta=0 \\ &f'=0, \theta=0 \text{ as } \eta\to\infty \end{aligned} \tag{2.11}$$

The solution of equations (2.7), (2.10) enable us to calculate the nondimensional velocity components $\bar{u}$, $\bar{v}$ from the following expressions

$$\begin{aligned} \bar{u} &= \frac{\nu^2}{Vg\beta(T_w-T_\infty)}u = \xi^2 f'(\xi,\eta) \\ \bar{v} &= \frac{\nu}{V} = \xi^{-1}(3f + \xi - \eta f' + \xi\frac{\partial f}{\partial \xi}) \end{aligned} \tag{2.12}$$

In practical applications, the physical quantities of principle interest are the shearing stress τ_w and the rate of heat transfer in terms of the skin-friction coefficients C_{fx} and Nusselt number Nu_x respectively, which can be written as

$$Nu_x = \frac{\nu}{V\Delta T}(q_c + q_r)_{\eta=0} and C_{fx} = \frac{V}{g\beta\Delta T}(\tau)_{\eta=0} \tag{2.13}$$

$$\text{where } \tau_w = \mu\left(\frac{\partial u}{\partial y}\right)_{\eta=0} \text{ and } q_c = -k\left(\frac{\partial T}{\partial y}\right)_{\eta=0} \tag{2.14}$$

q_r is the conduction heat flux.

Using the Equations (2.8) and the boundary condition (2.11) into (2.13) and (2.14), we get

$$\begin{aligned} C_{fx} &= \xi f''(x,0) \\ Nu_x &= -\xi^{-1}\left(1+\frac{4}{3}Rd\theta_w^3\right)\theta'(x,0) \end{aligned} \tag{2.15}$$

The values of the velocity and temperature distribution are calculated respectively from the following relations:

$$\bar{u} = \xi^2 f'(\xi,\eta), \quad \theta = \theta(x,y) \tag{2.16}$$

2.3 Results and discussion

In this exertion the effect of radiation on natural convection flow on a porous vertical plate in presence of heat generation is investigated. Solutions are obtained for fluids having Prandtl number Pr = 1.0 and for some test values of Pr = 0.8. 0.9, 1.0, 1.1 and 1.15 against η for a wide range of values of radiation parameter R_d, surface temperature parameter θ_w and heat generation parameter Q. We have considered the values of heat generation parameter Q = 00.0, 5.0, 10.0, 15.0 and 17.9 with radiation parameter R_d =0 1, Prandtl number Pr = 1.0 and surface temperature parameter θ_w = 1.1. The values of radiation parameter R_d =0 00, 0 05, 0.1, 0.2, and 0.3 have been taken while Q = 2.0, Pr = 1 0 and θ_w = 1.1. Different values of surface temperature parameter θ_w =0.0, 0.5. 1.5, 2.5, and 3 2.are considered while Q = 2.0, Pr = 1.0 and R_d =0.1. Numerical values of local rate of heat transfer are calculated in terms of Nusselt number Nu for the surface of the porous vertical plate from lower stagnation point to upper stagnation point. The effect for different values of heat generation parameter Q on local skin friction coefficient C_f and the local Nusselt number Nu, as well as velocity and temperature profiles with the Prandtl number Pr = 1.0, radiation parameter R_d =0.1 and surface temperature parameter θ_w = 1.1.

Figures 2.2-2.3 display results for the velocity and temperature profiles, for different values of heat generation parameter Q with Prandtl number Pr = 1.0, radiation parameter R_d =0.1 and surface temperature parameter θ_w = 1.1. It has been seen from Figures 2.2 and 2.3 that as the heat generation parameter Q increases, the velocity and the temperature profiles increase. The changes of velocity profiles in the η direction reveals the typical velocity profile for natural convection boundary layer flow. i.e., the velocity is zero at the boundary wall then the velocity increases to the peak value as η increases and finally the velocity approaches to zero (the asymptotic value).The maximum values of velocity are recorded to be 0 22590, 0.28724, 0.36866 and 0.46717 for Q=00.0, 5.0, 10.0, 15.0 respectively which occur at the same point η=0.83530 and for Q=17.9, the maximum values of velocity are recorded to be 0.53057. Here, it is observed that at η = 0.97931, the velocity increases by 106.8% as the heat generation parameter Q changes from 0.0 to 15.0. The changes of temperature profiles in the η direction also shows the typical temperature profile for natural convection boundary layer flow that is the value of temperature profile is 1.0 (one) at the boundary wall then the temperature profile decreases gradually along η

direction for the value Q -less then 1.0 to the asymptotic value. But for $Q \geq 1.0$ the temperature profile increases (at η = 0.68459 temperature is 2.20416 for Q = 17.9) and again it decreases gradually along η direction to the asymptotic value

The effect for different values of radiation parameter R_d the velocity and temperature profiles in case of Prandtl number Pr = 1.0, heat generation parameter Q = 2.0 and surface temperature parameter θ_w = 1.1 are shown in Figures 2.4 and 2.5. Here, as the radiation parameter Rd increases, the velocity profile increases and the temperature profile increases slightly such that there exists a local maximum of the velocity within the boundary layer, but velocity increases near the surface of the vertical porous plate and then temperature decreases and finally approaches to zero.

The effect of different values of surface temperature parameter θ_w, the velocity and temperature profiles while Prandtl number Pr = 1.0, heat generation parameter Q = 2.0 and radiation parameter R_d =0.1 are shown in Figures 2.6 and 2.7. Here, as surface temperature parameter θ_w increases, the velocity profile increases and the temperature profile increases such that there exists a local maximum of the velocity within the boundary layer, but velocity increases near the surface of the vertical porous plate and then temperature decreases and finally approaches to zero. However, in Figures 2.8 and 2.9, it is shown that when the Prandtl number Pr increases with θ_w = 1.1, R_d =0.1 and Q = 2.0, both the velocity and temperature profiles decrease.

Figures 2.10-2.11 show that skin friction coefficient C_f increases and heat transfer coefficient Nu decrease respectively for increasing values of heat generation parameter Q in case of Prandtl number Pr = 1.0, radiation parameter R_d =0.1 and surface temperature parameter θ_w = 1.1. The values of skin friction coefficient C_{fx} and Nusselt number Nu are recorded to be 0.18218, 0.17690, 0.16844, 0.16072, 0.15370 and 0.06579, 0.66612, 1.61572, 2.46974, 3.24161 for Q=17.9, 15.0, 10.0, 05.0 and 00.0 respectively which occur at the same point ξ = 0.23. Here, it is observed that at ξ = 0.23, the skin friction increases by 18.52% and Nusselt number Nu_x decreases by 97.336% as the heat generation parameter Q changes from 17.9 to 00.0. It is observed from the figure 2.10 that the skin friction increases gradually from zero value at lower stagnation point along the ξ direction and from Figure 2.11; it reveals that the rate of heat transfer decreases along the ξ direction from lower stagnation point to the upstream.

The effect of different values of radiation parameter R_d on the skin friction coefficient and the local rate of heat transfer while Prandtl number Pr = 1.0, heat generation parameter Q = 2.0 and surface temperature parameter θ_w = 1.1 are shown in the figures 2.12- 2.13. Here, as the radiation parameter R_d increases, the skin friction coefficient and heat transfer coefficient increase. From Figures 2.14 - 2.15, it can also easily be seen that an increase in the surface temperature parameter θ_w leads to increase in the local skin friction coefficient C_{fx} and the local rate of heat transfer Nu_x while Prandtl number Pr = 1.0, heat generation parameter Q = 2.0 and radiation parameter R_d =0.1. It is also observed that at any position of ξ, the skin friction coefficient C_{fx} increases and the local Nusselt number Nu_x increase as θ_w increases from 0.0 to 3.2. This phenomenon can easily be understood from the fact that when the surface temperature parameter θ_w increases, the temperature of the fluid rises and the thickness of the velocity boundary layer grows, i.e., the thermal boundary layer become thinner than the velocity boundary layer.

The variation of the local skin friction coefficient C_{fx} and local rate of heat transfer Nu_x for different values of Prandtl number Pr for θ_w = 1.1, Rd =0.1 and Q = 2.0 are shown in Figures 2.16 and 2.17. We can observe from these figures that as the Prandtl number Pr increases, the skin friction coefficient decreases and rate of heat transfer increase.

Numerical values of skin friction coefficient C_f and rate of heat transfer Nu are calculated from equations (2.15) and (2.16) for the surface of the porous plate from lower stagnation point at ξ= 0.01 to ξ=0.23. Numerical values of C_{fx} and Nu_x are depicted in Table 2.1.

Table 2. 1: Skin friction coefficient and rate of heat transfer against x for different values of heat generation parameter Q with other controlling parameters $Pr = 1.0$, $Rd = 0.1$, $\theta_w = 1.1$.

ξ	Q=00.00		Q=05.00		Q=15.00		Q=17.90	
	C_{fx}	Nu_x	C_{fx}	Nu_x	C_{fx}	Nu_x	C_{fx}	Nu_x
0.01000	0.00658	63.48390	0.00659	63.41941	0.00659	63.29037	0.00659	63.25294
0.02000	0.01316	31.79806	0.01316	31.70462	0.01318	31.51749	0.01318	31.46315
0.03000	0.01980	21.45338	0.01982	21.32936	0.01986	21.08118	0.01987	21.00816
0.04000	0.02636	16.15827	0.02640	16.00381	0.02648	15.69322	0.02651	15.60295
0.05000	0.03305	13.06291	0.03313	12.87776	0.03328	12.50441	0.03333	12.39560
0.06000	0.03960	10.94126	0.03973	10.72543	0.04000	10.28912	0.04008	10.16131
0.07000	0.04633	9.47057	0.04654	9.22375	0.04695	8.72285	0.04707	8.57579
0.08000	0.05289	8.33269	0.05319	8.05492	0.05381	7.48892	0.05399	7.32206
0.09000	0.05965	7.47655	0.06007	7.16749	0.06094	6.53465	0.06120	6.34736
0.10000	0.06622	6.76800	0.06679	6.42769	0.06798	5.72715	0.06834	5.51884
0.11000	0.07300	6.20876	0.07377	5.83677	0.07535	5.06650	0.07582	4.83626
0.12000	0.07958	5.72544	0.08056	5.32183	0.08262	4.48062	0.08324	4.22773
0.13000	0.08639	5.33190	0.08764	4.89618	0.09026	3.98158	0.09106	3.70489
0.14000	0.09297	4.98131	0.09453	4.51345	0.09783	3.52397	0.09883	3.22257
0.15000	0.09980	4.68956	0.10172	4.18914	0.10580	3.12176	0.10705	2.79424
0.16000	0.10639	4.42372	0.10872	3.89075	0.11371	2.74352	0.11525	2.38868
0.17000	0.11324	4.19896	0.11604	3.63276	0.12208	2.40231	0.12396	2.01846
0.18000	0.11984	3.99051	0.12316	3.39110	0.13041	2.07501	0.13268	1.66062
0.19000	0.12671	3.81216	0.13062	3.17888	0.13925	1.77308	0.14197	1.32608
0.20000	0.13331	3.64438	0.13788	2.97723	0.14807	1.47873	0.15131	0.99724
0.21000	0.14020	3.49949	0.14550	2.79773	0.15746	1.20180	0.16129	0.68326
0.22000	0.14680	3.36159	0.15292	2.62517	0.16687	0.92816	0.17138	0.37026
0.23000	0.15370	3.24161	0.16072	2.46974	0.17690	0.66612	0.18218	0.06579

Here in the above table the values of skin friction coefficient C_{fx} and Nusselt number Nu_x are recorded to be 0.18218, 0.17690, 0.16072, 0.15370 and 0.06579, 0.66612, 2.46974, 3.24161 for Q=17.9, 15.0, 10.0, 05.0 and 00.0 respectively which occur at the same point $\xi = 0.23$. Here, it is observed that at $\xi = 0.23$, the skin friction increases by 18.52% and Nusselt number Nu_x decreases by 97.336% as the heat generation parameter Q changes from 17.9 to 00.0.

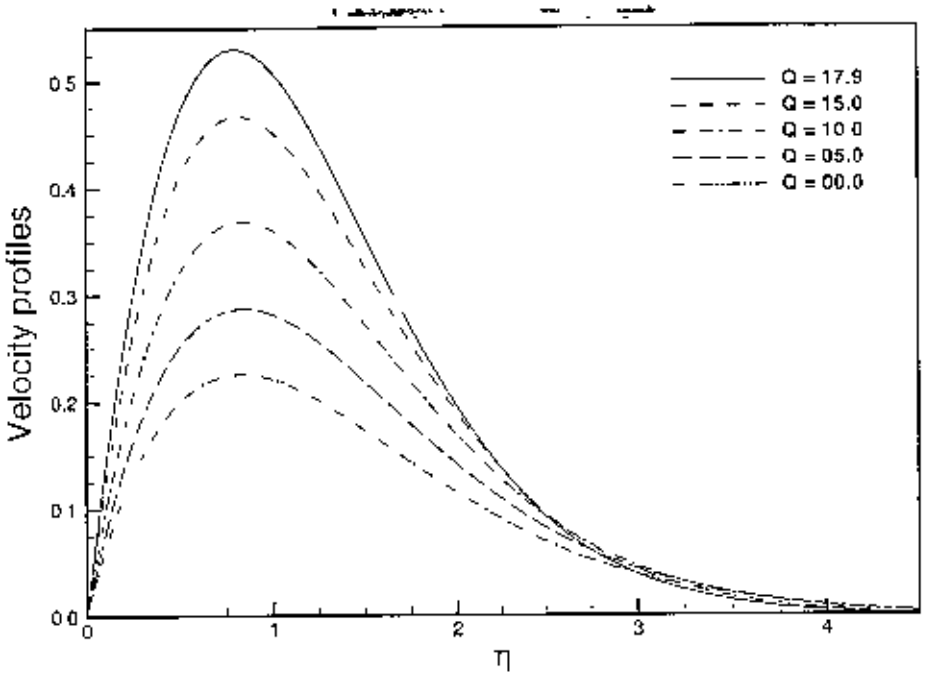

Figure 2.2: Velocity profiles for different values of Q with $Pr = 1.0$, $R_d = 0.1$ and $\theta_w = 1.1$

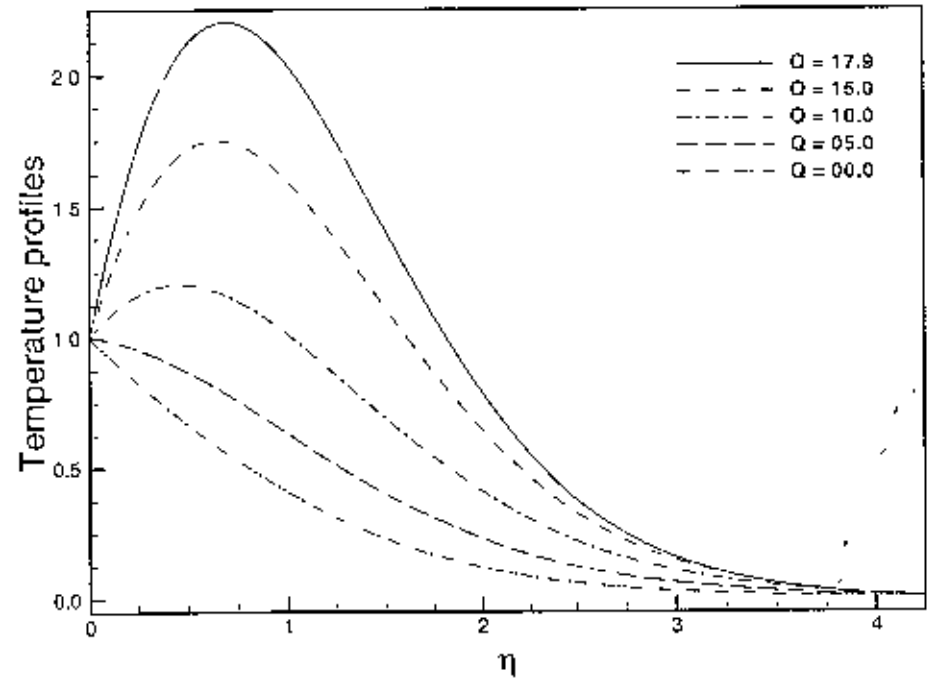

Figure 2.3: Temperature profiles for different values of Q with $Pr = 1.0$, $R_d = 0.1$ and $\theta_w = 1.1$

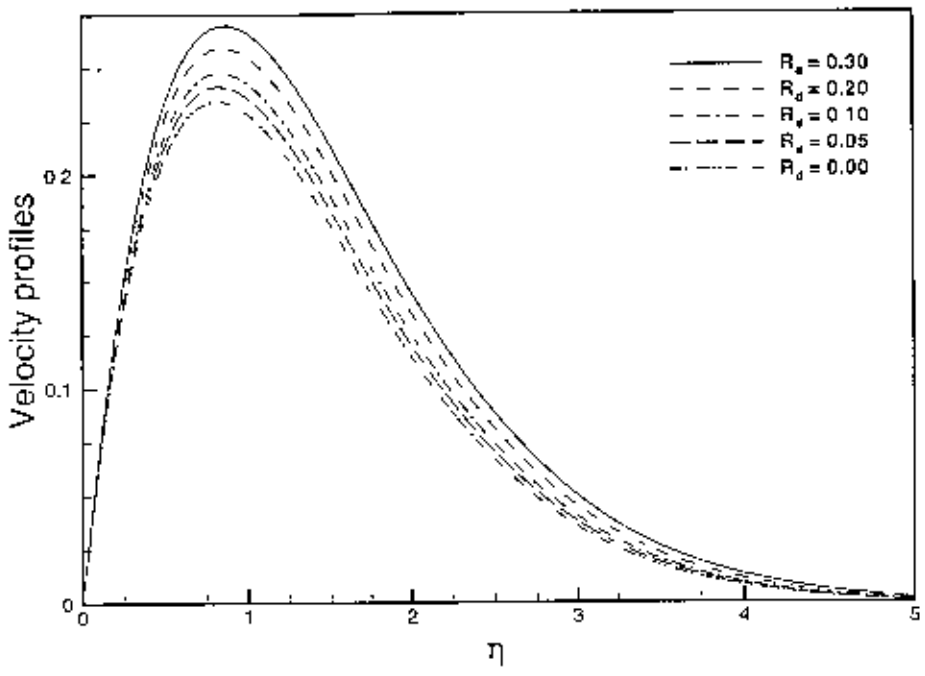

Figure 2.4: Velocity profiles for different values of R_d with Pr = 1.0, θw =1.1 and Q=2.0

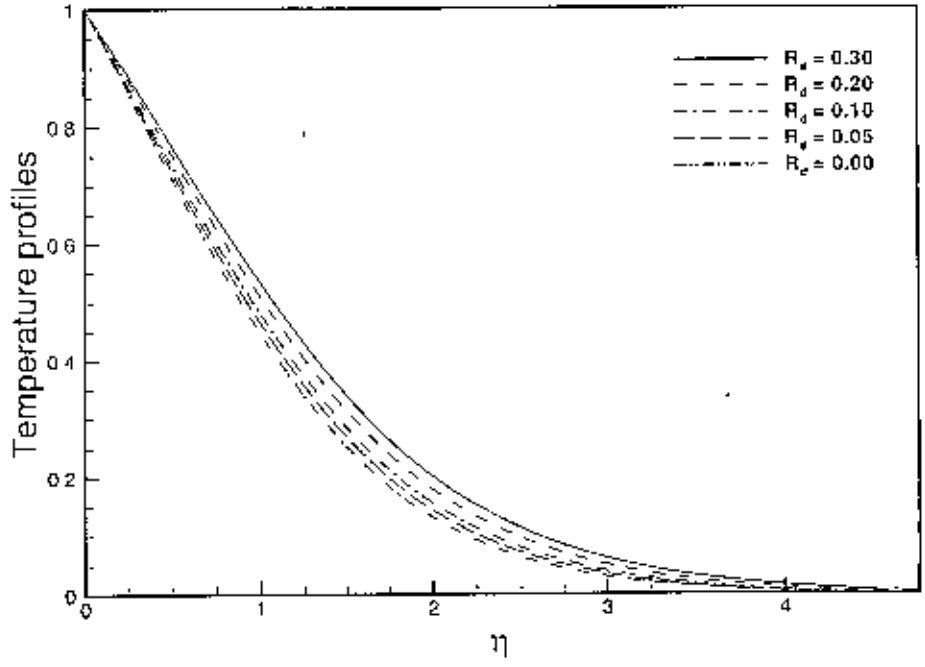

Figure 2.5: Temperature profiles for different values of R_d with Pr = 1.0, θ_w =1.1and Q=2.0

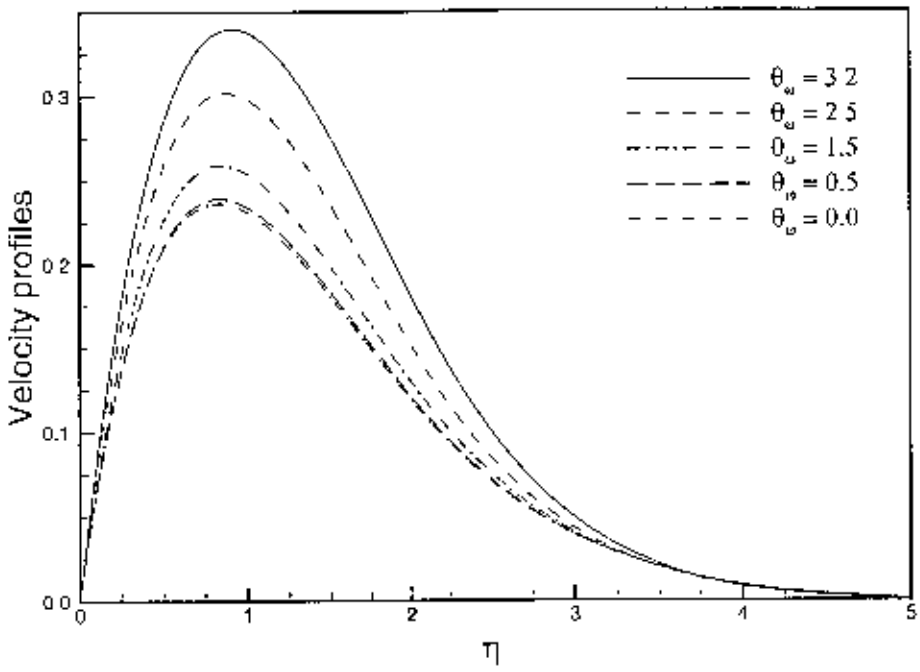

Figure 2.6: Velocity profiles for different values of θw with $Pr = 1.0$, R_d =0.1 and Q=2.0

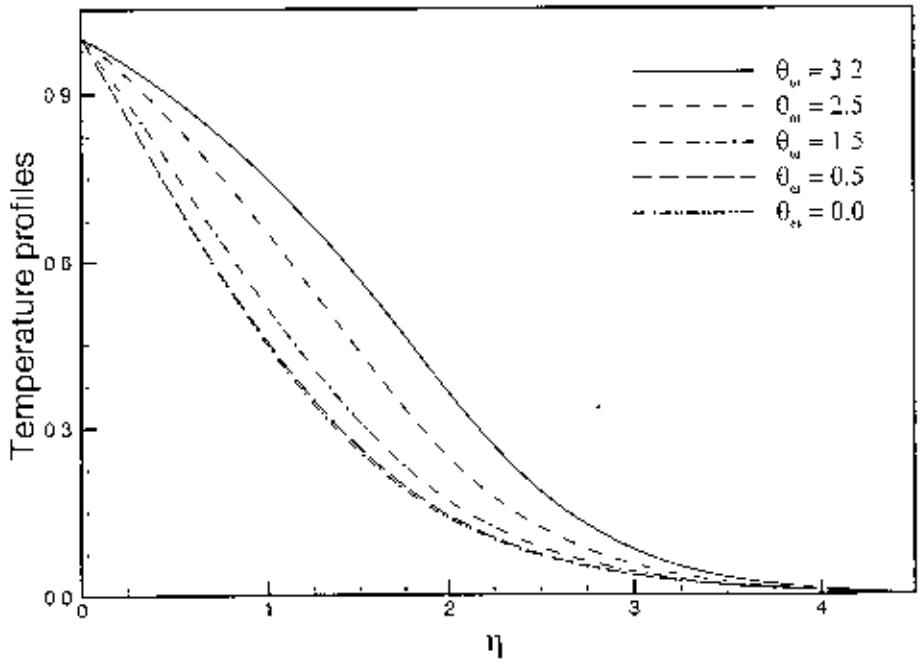

Figure 2.7: Temperature profiles for different values of θ_w with Pr = 1.0, R_d =0.1 and Q=2.0

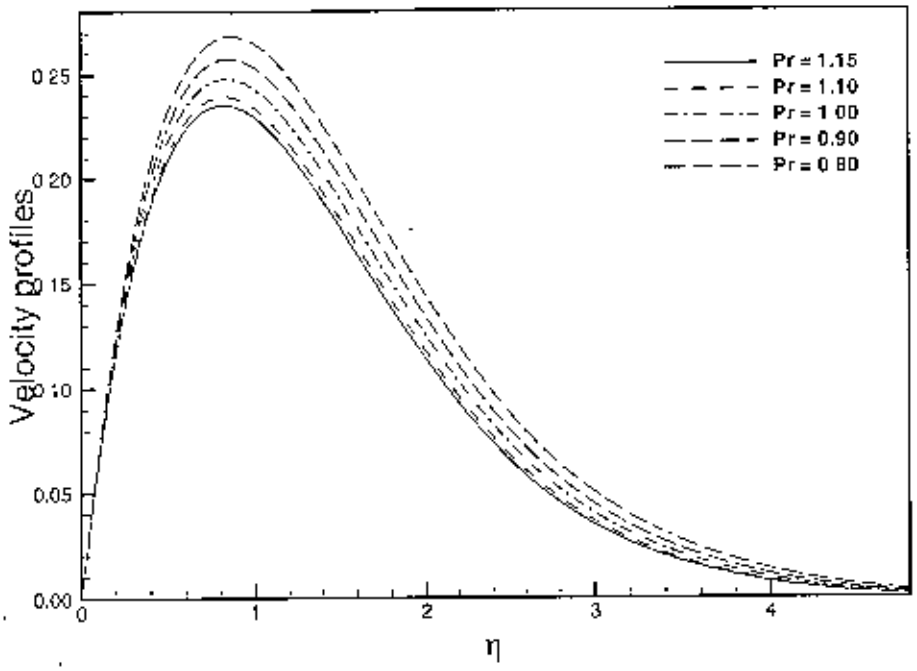

Figure 2.8: Velocity profiles for different values of Pr with R_d =0.1, θ_w =1.1and Q=2.0

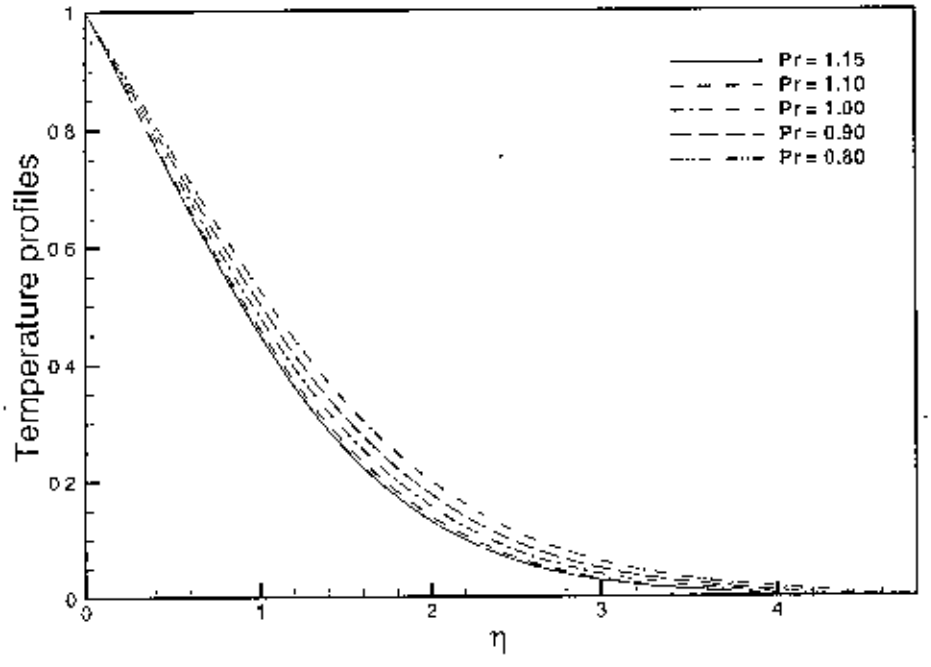

Figure 2.9: Temperature profiles for different values of Pr with R_d =0.1, θ_w =1.1and Q=2.0

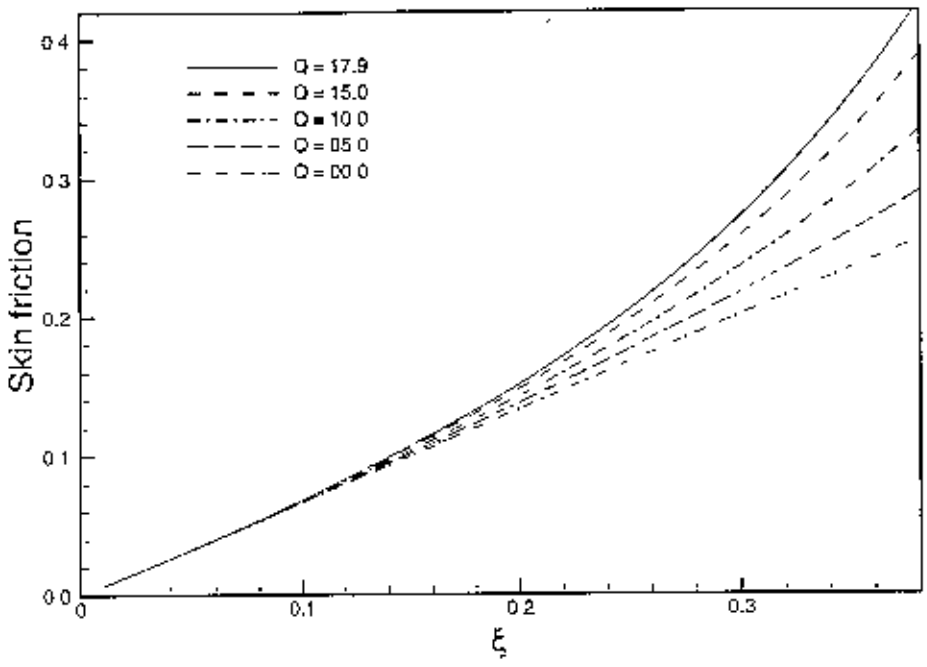

Figure 2.10: Skin-friction coefficient for different values of Q with $Pr = 1.1$, $R_d = .1$ and $\theta_w = 1.5$

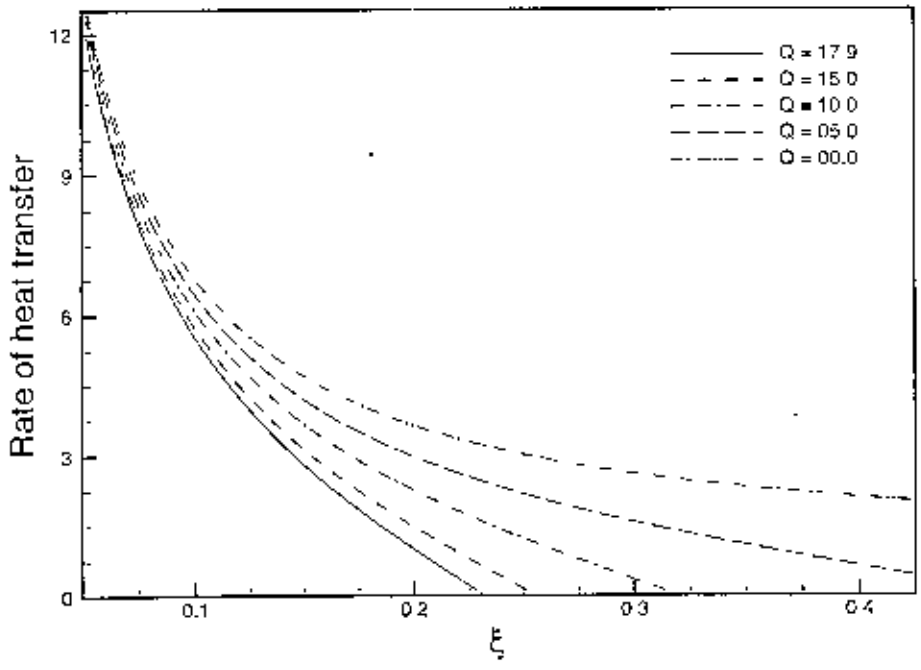

Figure 2.11: Rate of heat transfer for different values of Q with $Pr = 1.0$ $R_d = 0.1$ and $\theta w = 1.1$

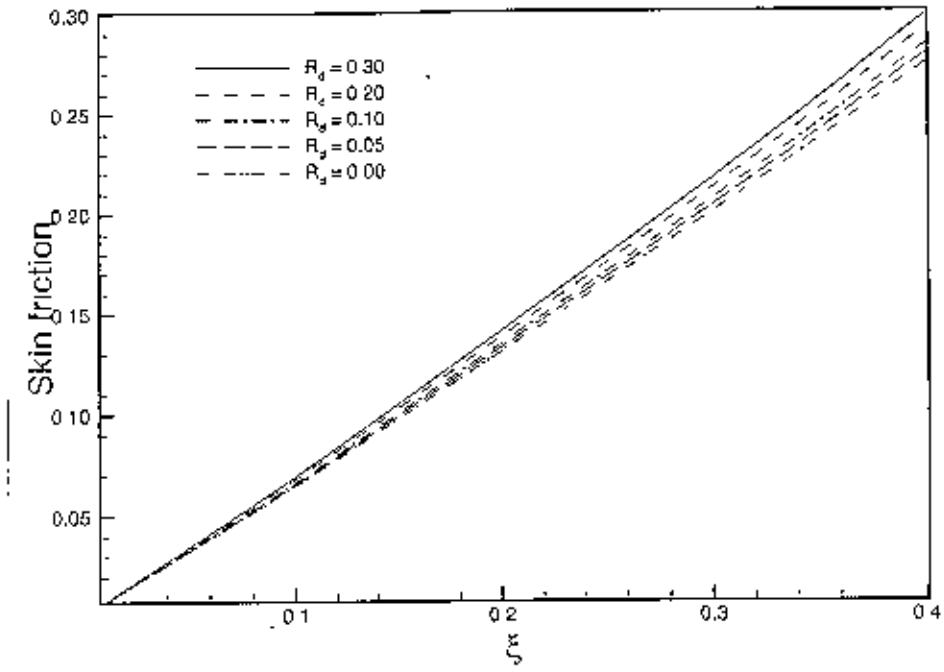

Figure 2.12: Skin-friction coefficient for different values of R_d with $Pr = 1.1$, $\theta_w = 1.5$ and $Q=2.0$

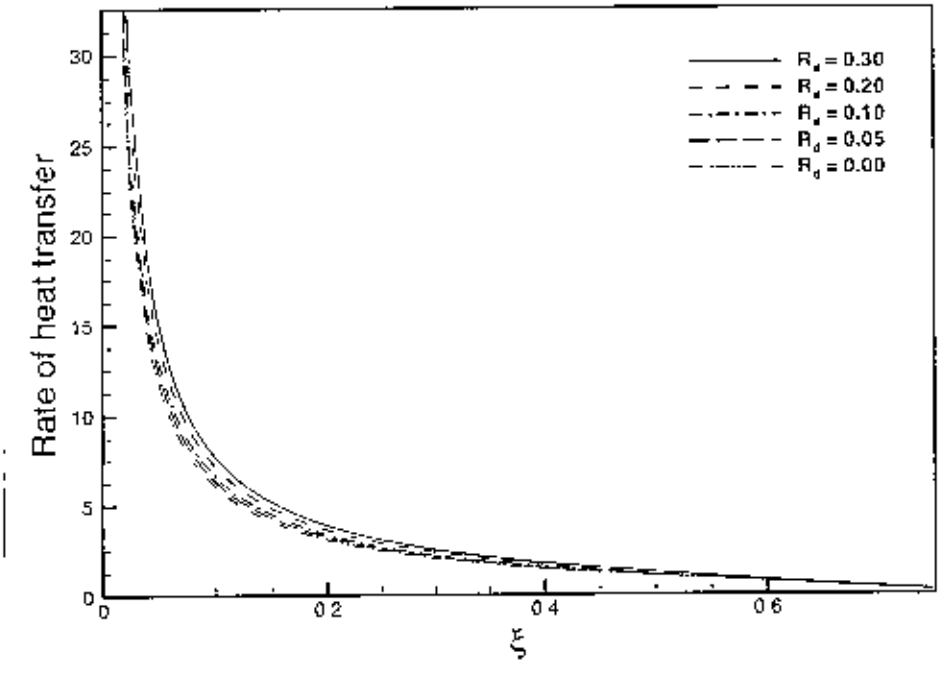

Figure 2.13: Rate of heat transfer for different values of R_d with Pr = 1.0 θw =1.1and Q=2.0

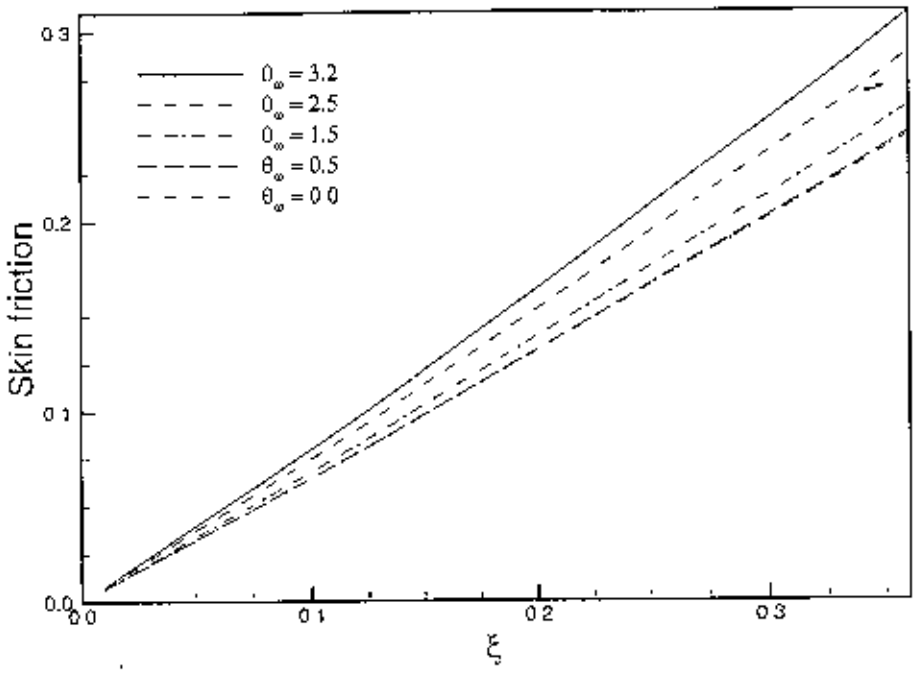

Figure 2.14: Skin-friction coefficient for different values of θ_w with $Pr = 1.0$ $R_d = 0.1$ and $Q = 2.0$

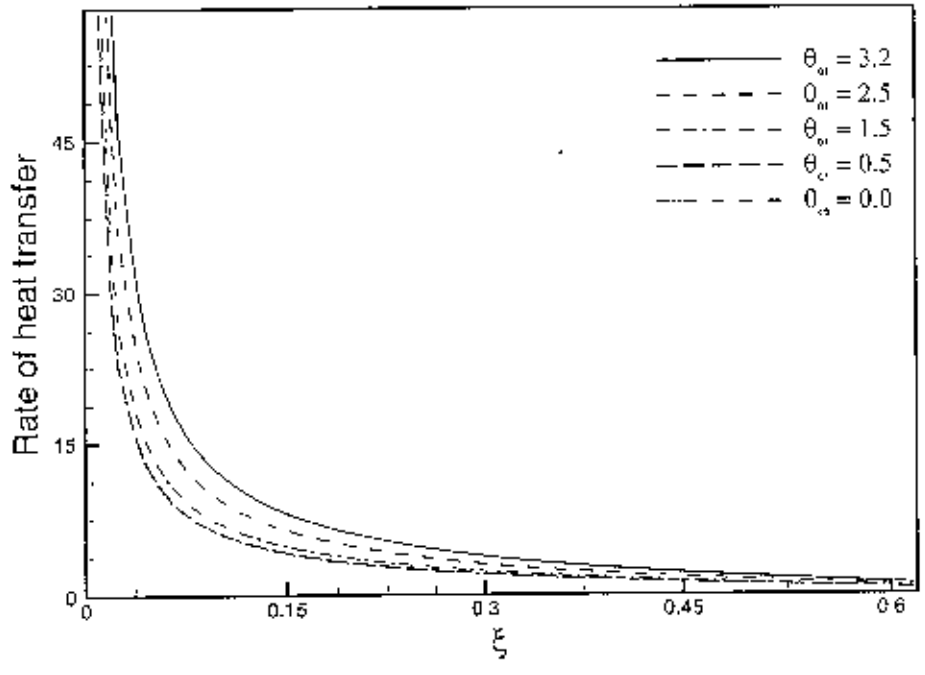

Figure 2.15: Rate of heat transfer for different values of θ_w with $Pr = 1.0$, $R_d = 0.1$ and $Q = 2.0$

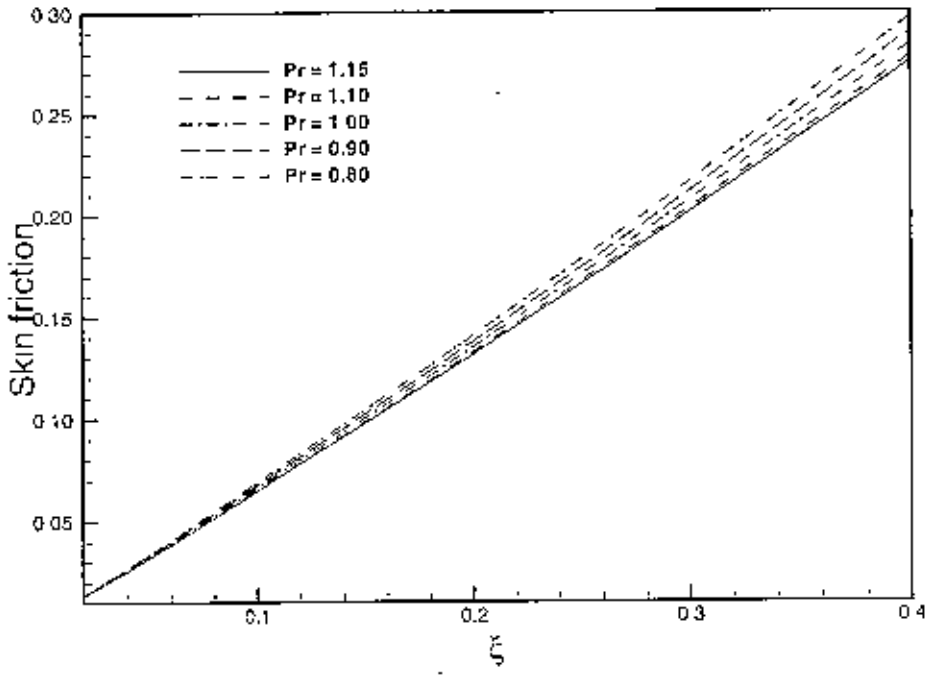

Figure 2.16: Skin-friction coefficient for different values of *Pr* with R_d =0.1, θ_w =1.1 and Q=2.0

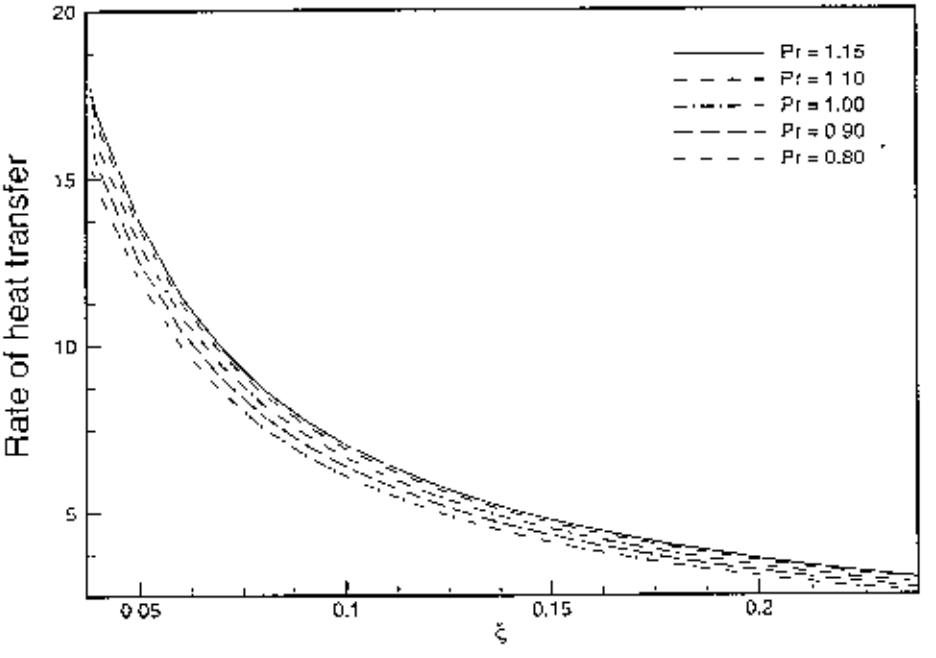

Figure 2.17: Rate of heat transfer for different values of *Pr* with R_d =0.1, θ_w =1.1 and Q=2.0

2.4 Conclusion

The effect of radiation on natural convection flow on a porous vertical plate in presence of heat generation has been investigated for different values of relevant physical parameters including Prandtl number Pr, and surface temperature parameter θ_w.

- Significant effects of heat generation parameter Q on velocity and temperature profiles as well as on skin friction and the rate of heat transfer have been found in this investigation but the effect of heat generation parameter Q on rate of heat transfer is more significant. An increase in the values of heat generation parameter Q leads to increase both the velocity and the temperature profiles, the local skin friction coefficient C_{fx} increases at different position of η and the local rate of heat transfer Nu_x decreases at different position of ξ for $\xi < 0.1$ and decrease asymptotically when $Pr = 1.0$.
- The increase in the values of radiation parameter R_d leads to increase in the velocity profile, the temperature profile, the local skin friction coefficient C_{fx} and the local rate of heat transfer Nu_x.
- All the velocity profile, temperature profile, the local skin friction coefficient C_{fx} and the local rate of heat transfer Nu_x increases significantly when the values of surface temperature parameter θ_w increase.
- The increase in Prandtl number Pr leads to decrease in all the velocity profile, the temperature profile, the local skin friction coefficient C_{fx} but the local rate of heat transfer Nu_x increase.

Chapter 3

Effect of Radiation on Magnetohydrodynamic Natural Convection Flow from a porous vertical plate in Presence of Heat Generation

3.1 Introduction

This chapter describes the effect of radiation on Magnetohydrodynamic (MHD) natural convection flow from a porous vertical plate in presence of heat generation. The governing boundary layer equations are first transformed into a non-dimensional form and the resulting nonlinear system of partial.differential equations are then solved numerically using a very efficient finite-difference method known as the Keller-box scheme. Here the attention has given on the evolution of the surface shear stress in terms of local skin friction and the rate of heat transfer in terms of local Nusselt number, velocity distribution as well as temperature distribution for a selection of parameters set consisting of heat generation parameter, magnetohydrodynamic (MHD) parameter and the Prandlt number.

3.2 Formulation of the problem:

Magnetohydrodynamic (MHD) natural convection boundary layer flow from a porous vertical plate of a steady two dimensional viscous incompressible fluid in presence of heat generation and radiation heat transfer has been investigated. It is assumed that the surface temperature of the porous vertical plate, T_w, is constant, where $T_w > T_\infty$ Here T_∞ is the ambient temperature of the fluid, T is the temperature of the fluid in the boundary layer, g is the acceleration due to gravity, the fluid is assumed to be a grey emitting and absorbing, but non scattering medium.In the present work following assumptions are made:

i) Variations in fluid properties are limited only to those density variations which affect the buoyancy terms

ii) Viscous dissipation effects are negligible and

iii) The radiative heat flux in the x-direction is considered negligible in comparison with that in the y direction, where the physical coordinates (u, v) are velocity components along the (x, y)axes. The physical configuration considered is as shown in Fig.3.1:

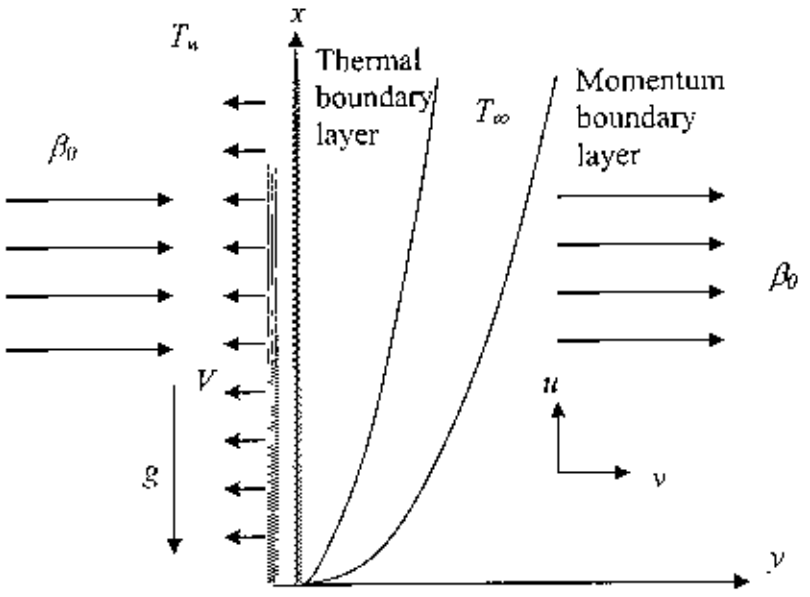

Figure: 3.1The coordinate system and the physical model

Under the usual Boussinesq approximation, the continuity, momentum and energy equations for two dimensional steady laminar boundary layer flow problem under consideration can be written:

$$\frac{\partial u}{\partial x}+\frac{\partial v}{\partial y}=0 \tag{3.1}$$

$$\rho\left(u\frac{\partial u}{\partial x}+v\frac{\partial u}{\partial y}\right)=\mu\frac{\partial^2 u}{\partial x^2}+\rho g\beta(T-T_\infty)-\sigma_0\beta_0^2 u \tag{3.2}$$

$$\rho c_p\left(u\frac{\partial T}{\partial x}+v\frac{\partial T}{\partial y}\right)=k\frac{\partial^2 T}{\partial y^2}-\frac{\partial q_r}{\partial y}+Q_0(T-T_\infty) \tag{3.3}$$

With the boundary conditions

$$\begin{aligned} &x=0, y>0, u=0, T=T_\infty, \\ &y=0, x>0, u=0, v=V\ T=T_w \\ &y\to\infty, x>0, u=0, T=T_\infty \end{aligned} \tag{3.4}$$

where ρ is the density, k is the thermal conductivity, β is the coefficient of thermal expansion, ν is the reference kinematic viscosity $\nu=\mu/\rho$, μ is the viscosity of the fluid, C_p is the specific heat due to constant pressure and q_r is the radiative heat flux in the y direction, β_0 is the strength of magnetic field, σ_0 is the electrical conduction. In order to reduce the complexity of the problem and to provide a means of comparison with future

studies that will employ a more detail representation for the radiative heat flux; we will consider the optically thick radiation limit. Thus radiation heat flux term is simplified by the Rosseland diffusion approximation [Özisik (1973)] and is given by

$$q_r = -\frac{4\sigma}{3(a_r + \sigma_s)}\frac{\partial T^4}{\partial y} \tag{3.5}$$

In Equation (3.5) a_r is the Rosseland mean absorption co-efficient, σ_s is the scattering co-efficient and σ is the Stephan-Boltzman constant.

Now introduce the following non-dimensional variables:

$$\eta = \frac{y}{\xi} \tag{3.6}$$

$$\xi = \nu\left\{\frac{4x}{\nu^2 g\beta\Delta T}\right\}^{\frac{1}{4}} \tag{3.7}$$

$$\psi = \nu^{-1}\nu^2 g\beta\Delta T\xi^3\left\{f + \frac{\xi}{4}\right\}$$

$$\theta = \frac{T - T_\infty}{T_w - T_\infty}, \tag{3.8}$$

$$\theta_w = \frac{T_w}{T_w}, \quad \Lambda = \theta_w - 1 = \frac{T_w}{T_\infty} - 1 = \frac{T_w - T_\infty}{T_\infty}, \quad Rd = \frac{4\sigma T_\infty^3}{k(a+\sigma_s)}$$

Where, θ is the non-dimensional temperature function, θ_w is the surface temperature parameter and R_d is the radiation parameter.

Substituting (3.8) into Equations (3.1), (3.2) and (3.3) leads to the following non-dimensional equations

$$f''' + \theta - 2f'^2 + 3ff'' + \xi f'' = \xi\left(f'\frac{\partial f'}{\partial \xi} - f''\frac{\partial f'}{\partial \xi}\right) - \frac{\sigma_0\beta_0^2}{\rho}\nu^{-2}\xi^2 f' \tag{3.9}$$

$$\frac{1}{Pr}\frac{\partial}{\partial \eta}\left[\left\{1 + \frac{4}{3}Rd\left(1 + (\theta_w - 1)\theta\right)^3\right\}\frac{\partial \theta}{\partial \eta}\right] + Q\theta + 3f\theta' + \xi\theta' = \xi\left(f'\frac{\partial \theta}{\partial \xi} - \frac{\partial f}{\partial \xi}\theta'\right) \tag{3.10}$$

where $Pr = \nu C_p/k$ is the Prandtl number, $Q = \nu Q_0\xi^2/\nu^2\rho C_p$ is the heat generation parameter and $M = \beta_0^2\sigma_0/\nu\rho$ is the magneto hydrodynamic parameter.

The boundary conditions (3.4) become

$$f = 0, f' = 0, \ \theta = 1 \ \text{at} \ \eta = 0$$
$$f' = 0, \ \theta = 0 \ \text{as} \ \eta \to \infty \tag{3.11}$$

The solutions of equations (3.9), (3.10) and (3.11) enable us to calculate the nondimensional velocity components $\bar{u}, \bar{v}$ from the following expressions

$$\begin{aligned} \bar{u} &= \frac{\nu^2}{Vg\beta(T_w - T_\infty)}u \\ &= \xi^2 f'(\xi,\eta) \\ \bar{v} &= \frac{\nu}{V} \\ &= \xi^{-1}\left(3f + \xi - \eta f' + \xi\frac{\partial f}{\partial \xi}\right) \end{aligned} \tag{3.12}$$

In practical applications, the physical quantities of principle interest are the shearing stress τ_w and the rate of heat transfer in terms of the skin-friction coefficients C_{f_x} and Nusselt number Nu_x respectively, which can be written as

$$Nu_x = \frac{\nu}{V\Delta T}(q_c + q_r)_{\eta=0} \text{ and } C_{fx} = \frac{\nu}{g\beta\Delta T}(\tau)_{\eta=0} \tag{3.13}$$

$$\text{where} \quad \tau_w = \mu\left(\frac{\partial \hat{u}}{\partial \hat{y}}\right)_{\eta=0} \quad \text{and} \quad q_c = -k\left(\frac{\partial T}{\partial \hat{y}}\right)_{\eta=0}, \tag{3.14}$$

q_c is the conduction heat flux

Using the Equations (3.8) and the boundary condition (3.11) into (3.13) and (3.14),we get

$$\begin{aligned} C_{f_x} &= \xi f''(x,0) \\ Nu_x &= \xi^{-1}\theta'(x,0) \end{aligned} \tag{3.15}$$

The values of the velocity and temperature distribution are calculated respectively from the following relations:

$$\bar{u} = \xi^2 f'(\xi,\eta), \quad \theta = \theta(x,y) \tag{3.16}$$

We discuss velocity distribution as well as temperature profiles for a selection of parameter sets consisting of heat generation parameter, MHD parameter, and the Prandlt number at different position of ξ.

3.3 Results and discussion

In this context we have investigated analytically the effect of radiation on magnetohydrodynamic natural convection flow on a porous vertical plate in presence of heat generation. Solutions are obtained for fluids having Prandtl number Pr = 1.0 and for some values of Pr = 0.8, 0.9, 1.0, 1.1 and 1.15 against η for a wide range of values of radiation parameter R_d, surface temperature parameter θ_w, heat generation parameter Q and magnetic parameter M. We have considered the values of heat generation parameter Q = 0.0, 5 0, 10.0, 15 0 and 17.9 with radiation parameter R_d=0.1, Prandtl number Pr = 1.0 and surface temperature parameter θ_w = 1.1 and magnetic parameter M=2.0. The values of radiation parameter R_d =0.0, 0.05, 0.1, 0.2 and 0 .3 have been taken in case of Q = 2.0, Pr = 1.0, θ_w = 1.1 and magnetic parameter M=2.0. The different values of surface temperature parameter θ_w = 0 0, 0.5, 1.5, 2.5 and 3.2 are considered with Q = 2.0, Pr = 1.0 and R_d =0.1 and M=2 0. Different values of magnetic parameter M=0 0, 5.0, 10.0. 15.0 and 25.0 have been taken in case of Q = 2.0, Pr = 1.0, θ_w = 1.1 and R_d =0 1 Numerical values of local rate of heat transfer are calculated in terms of Nusselt number Nu for the surface of the porous plate from lower stagnation point to upper stagnation point. The effect for different values of heat generation parameter Q and magnetic parameter M on local skin friction coefficient C_{fx} and the local Nusselt number Nu_x, as well as velocity and temperature profiles with the Prandtl number Pr = 1.0, radiation parameter R_d =0.1 and surface temperature parameter θ_w = 1.1, are also observed.

Figures 3.2-3.3 display results for the velocity and temperature profiles, for different values of heat generation parameter Q while Prandtl number Pr = 1.0, radiation parameter R_d =0.1 surface temperature parameter θ_w = 1.1 and magnetic parameter M=2.0. It has been seen from Figures 3.2 and 3.3 that as the heat generation parameter Q increases, the velocity profiles decreases and the temperature profiles increase. The changes of velocity profiles in the η direction reveals the typical velocity profile for natural convection boundary layer flow, i.e., the velocity is zero at the boundary wall then the velocity increases to the peak value as η increases and finally the velocity approaches to zero (the asymptotic value). The changes of temperature profiles in the η direction also shows the typical temperature profiles for natural convection boundary layer flow that is the value of temperature profiles is 1.0 (one) at the boundary wall then the temperature profile increases for η<1 and decreases gradually along $\eta \geq 1$ direction to the asymptotic value.

The variation of the velocity and temperature profiles for different values of radiation parameter R_d in case of surface temperature parameter $\theta_w = 1.1$, Prandtl number $Pr = 1.0$, heat generation parameter $Q = 2.0$ and magnetic parameter $M=2.0$ are shown in Figures 3.4 and 3.5. Here, as the radiation parameter R_d increases, both the velocity and the temperature profiles increase slightly such that there exists a local maximum of the velocity within the boundary layer, but velocity increases near the surface of the vertical porous plate and then temperature decreases slowly and finally approaches to zero.

The effect for different values of surface temperature parameter θ_w, the velocity and temperature profiles with Prandtl number $Pr = 1.0$, heat generation parameter $Q = 2.0$, radiation parameter $R_d = 0.1$ and magnetic parameter $M=2.0$ are shown in Figures 3.6 and 3.7. Here, as the surface temperature parameter θ_w increases, the velocity and the temperature profiles increase slightly such that there exists a local maximum of the velocity within the boundary layer, but velocity increases near the surface of the porous plate and then temperature decreases slowly and finally approaches to zero. However, in figures 3.8 and 3.9 it has been shown that when the Prandtl number $Pr = 0.8, 0.9, 1.0, 1.1$ and 1.15 increases with $\theta_w = 1.1$, $R_d = 0.1$, $Q = 2.0$ and $M=2.0$, both the velocity and temperature profiles decrease.

Figures 3.10 display results for the velocity profiles for different values of magnetic parameter M with Prandtl number $Pr = 1.0$, radiation parameter $R_d = 0.1$, heat generation parameter $Q = 2.0$ and surface temperature parameter $\theta_w = 1.1$. It has been seen from figure 3.10 that as the magnetic parameter M increases, the velocity profiles increase up to the position of $\eta=0.73363$ after that position velocity profiles decrease with the increase of magnetic parameter. It is also observed from figure 3.10 that the changes of velocity profiles in the η direction reveals the typical velocity profile for natural convection boundary layer flow, i.e., the velocity is zero at the boundary wall then the velocity increases to the peak value as η increases and finally the velocity approaches to zero (the asymptotic value) but we see from this figure and its magnified portion for M=25.0 the velocity profile crosses all the other velocity profiles. This is because of the velocity profiles having lower peak values for higher values of magnetic parameter tend to increase comparatively slower along η direction than velocity profiles with higher peak values for lower values of magnetic parameter. Figure 3.11 display results for the temperature profiles, for different values of magnetic parameter M while Prandtl number $Pr = 1.0$,

radiation parameter R_d =0.1, heat generation parameter Q = 2.0 and surface temperature parameter θ_w = 1.1. The maximum values of velocity are recorded to be 0.69695, 0.46467, 0.36407, 0.28047 and 0.21740 for M=.25.0, 20.0, 10.0, 5.0, and 0.0, at η=0.73363, η=0.83530 and η=0.99806. The velocity is 0.45019 at η=0.99806 for M =25.0. Here, it is observed that at η=0.99806, the velocity increases by 108.32% as the magnetic parameter M changes from 0 to 25.0.

From figure 3.11, as the magnetic parameter M increases, the temperature profiles increase. we observed that the temperature profile is 1.0 (one) at the boundary wall then the temperature profile decreases gradually along η direction to the asymptotic value. But for M=25.0 the temperature profile increases, at η=0.63635 it is 1.79070 then it decrease.

Figure 3.12 show that skin friction coefficient C_{fx} decreases for increasing values of heat generation parameter Q with Prandtl number Pr = 1.0, radiation parameter R_d =0.1, surface temperature parameter θ_w = 1.1 and magnetic parameter M=2.0. It is observed from Figure 3.12 that the skin friction increases gradually from zero value at lower stagnation point along the ξ direction and from Figure 3.13; it reveals that the rate of heat transfer increases along the ξ direction. But for Q=0.0, 5.0 and 10.0 Nu_x are along ξ axis.

The effect for different values of radiation parameter R_d , the skin friction coefficient and heat transfer coefficient while Prandtl number Pr = 1.0, heat generation parameter Q = 2.0, surface temperature parameter θ_w= 1.1 and magnetic parameter M=2.0 are shown in Figures 3.14- 3.15. Here, as the radiation parameter Rd increases, both the skin friction coefficient and heat transfer coefficient increase.

From Figures 3.16 - 3.17, it can also easily be seen that an increase in the surface temperature parameter θ_w leads to increase in the local skin friction coefficient C_f and heat transfer coefficient increase while Prandtl number Pr = 1.0, heat generation parameter Q = 2.0, radiation parameter R_d =0.1 and magnetic parameter M=2.0. This phenomenon can easily be understood from the fact that when the surface temperature parameter θ_w decreases, the temperatures of the fluid decline and the thickness of the velocity boundary layer downhill, i.e., the thermal boundary layer becomes thicker than the velocity boundary layer. Therefore the skin friction coefficient C_{fx} and the local Nusselt number Nu_x drops off.

The variation of the local skin friction coefficient C_f and local rate of heat transfer Nu for different values of Prandtl number Pr while $\theta_w = 1.1$, $R_d = 0.1$, $Q = 2.0$ and $M=2.0$ are shown in Figures 3.18 and 3.19. We can observe from these figures that as the Prandtl number Pr increases, the skin friction coefficient decreases and rate of heat transfer increases.

Figures 3.20-3.21 show that skin friction coefficient C_{fx} and heat transfer coefficient Nu_x decreases for increasing values of magnetic parameter M while heat generation parameter $Q=2.0$..Prandtl number $Pr = 1.0$, radiation parameter $R_d = 0.1$ and surface temperature parameter $\theta_w = 1.1$. The values of skin friction coefficient C_{fx} and Nusselt number Nu_x are recorded to be 0.14845, 0.13862, 0.13416, 0.12997 and 0.12605 and 0.12212, 1.75442, 2.48459, 3.16466 and 3.79971 for M=25.0, 15.0.10.0, 5.0 and.0.0 respectively which occur at the same point $\xi = 0.19$. Here, it observed that at $\xi = 0.19$, the skin friction increases by 17.7% and Nusselt number Nu_x decreases by 96.17% as the magnetic parameter M changes from 0.0 to 25.0. It is observed from figure 3.20 that the skin friction increases gradually from zero value at lower stagnation point along the ξ direction and from Figure 3.21; it reveals that the rate of heat transfer decreases along the ξ direction.

Numerical values of rate of heat transfer Nu_x and skin friction coefficient C_f are calculated from Equations (3.15) and (3.16) from the surface of the vertical porous plate. Numerical values of C_{fx} and Nu_x are shown in table 3.1.

Table 3.1: Skin friction coefficient and rate of heat transfer against x for different values of magnetic parameter M with other controlling parameters $Pr = 1.1$, $Rd = 0.1$, $\theta_w = 1.5$ and $Q = 2.0$.

ξ	M=00.0		M=05.0		M=15.0		M=25.0	
	C_{fx}	Nu_x	C_{fx}	Nu_x	C_{fx}	Nu_x	C_{fx}	Nu_x
0 01000	0.00658	63.48268	0 00659	63 41818	0.00659	63 28914	0.00659	63 16005
0 02000	0.01315	31 79624	0.01316	31.70281	0 01317	31.51566	0.01319	31 32832
0.03000	0.01980	21 45096	0.01982	21.32690	0.01985	21.07806	0 01989	20.82805
0.04000	0 02635	16.15525	0.02639	16 00079	0.02647	15 68825	0 02656	15.37767
0.05000	0 03303	13.05928	0.03311	12.87407	0.03327	12.50024	0.03343	12 12365
0.06000	0.03958	10 93702	0.03971	10.72112	0.03998	10.28547	0.04025	9.84166
0.07000	0.04629	9 46571	0.04650	9.21878	0.04692	8.71719	0.04734	8.20672
0.08000	0 05284	8.32719	0.05314	8.04930	0.05376	7.48339	0 05439	6.90212
0.09000	0 05958	7.47044	0.06000	7.16120	0.06087	6.52766	0.06177	5.87421
0.10000	0 06612	6.76127	0.06670	6 42070	0.06789	5 71982	0.06912	4 99045
0.11000	0 07287	6.20139	0.07364	5 82907	0.07522	5 05786	0.07688	4 24959
0.12000	0 07941	5.71745	0.08040	5 31340	0.08246	4.47137	0.08463	3 58008
0.13000	0.08617	5.32327	0 08743	4.88739	0 09005	3.97100	0 09285	2.99239
0.14000	0.09270	4.97206	0 09427	4.50378	0 09757	3.51256	0 10111	2.44167
0 15000	0.09948	4.67968	0.10140	4.17830	0 10548	3.10891	0 10992	1 94003
0.16000	0.10600	4.41320	0.10833	3 87915	0.11333	2 72959	0.11882	1.45658
0.17000	0.11277	4.18780	0.11557	3 62029	0.12163	2 38680	0.12835	1.00226
0.18000	0.11928	3.97871	0.12261	3.37780	0.12987	2.05815	0.13804	0.55441
0.19000	0.12605	3 79971	0.12997	3.16466	0.13862	1.75442	0.14845	0.12212

In ths above table the values of skin friction coefficient C_{fx} and Nusselt number Nu_x are recorded to be 0 14845, 0.13862, 0.12997 and 0 12605 and 0.12212, 1.75442. 3.16466 and 3.79971 for M=25.0, 15 0.10.0, 5.0 and.0.0 respectively which occur at the same point ξ = 0.19. Here, it observed that at $\xi = 0.19$, the skin friction increases by 17.7% and Nusselt number Nu_x decreases by 96.17% as the magnetic parameter M changes from 0.0 to 25.0.

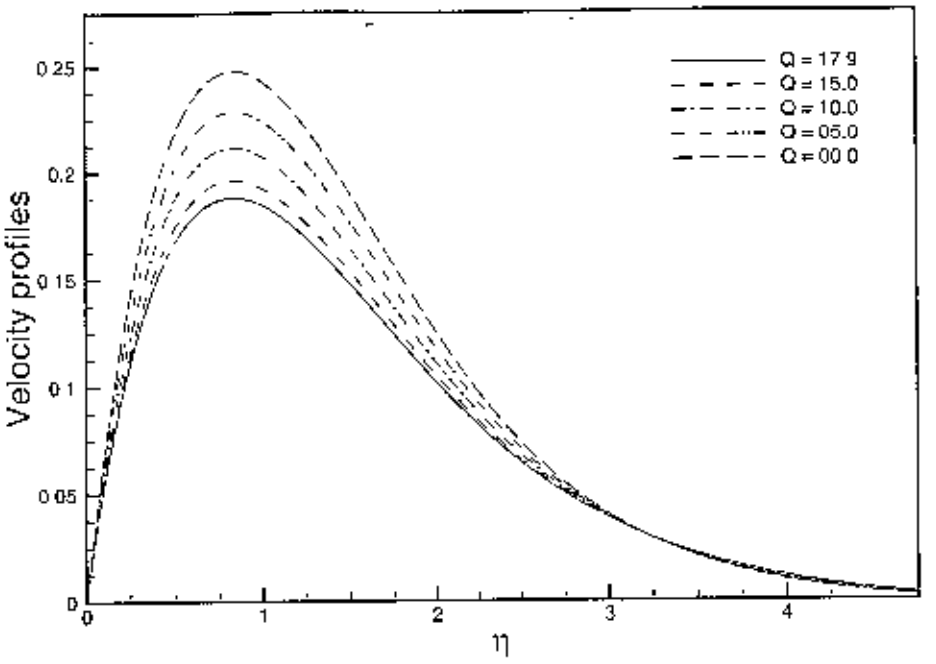

Figure 3.2: Velocity profiles for different values of Q in case of Pr = 1.0, R_d =0.1, θ_w = 1.1 and M.= 2.0

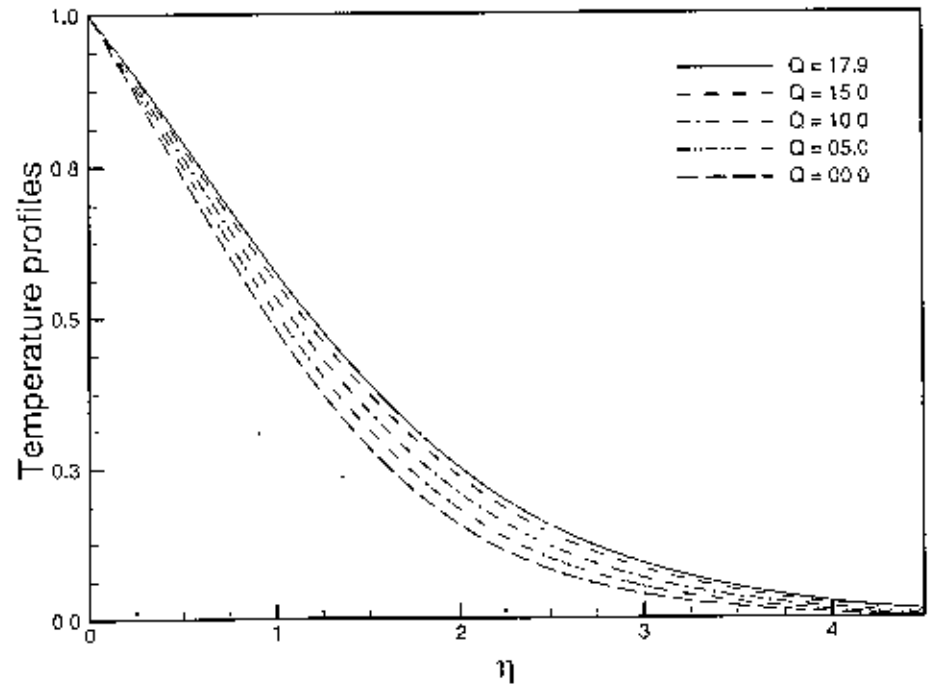

Figure 3.3: Temperature profiles for different values of Q in case of Pr = 1.0, R_d =0.1, θ_w = 1.1 and M= 2.0

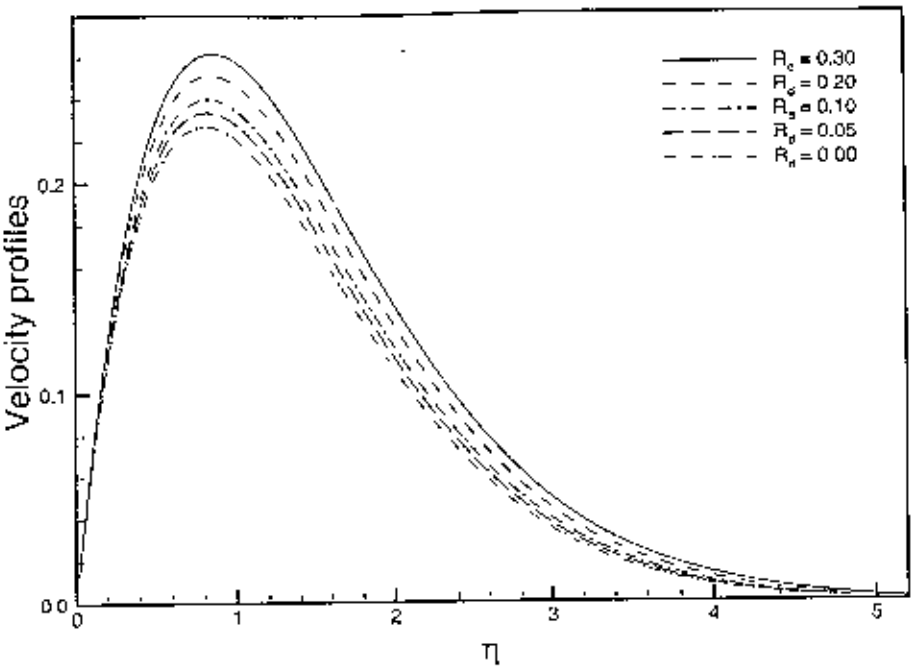

Figure 3.4: Velocity profiles for different values of R_d in case of Pr = 1.0, Q=2.0, θ_w = 1.1 and M. = 2.0

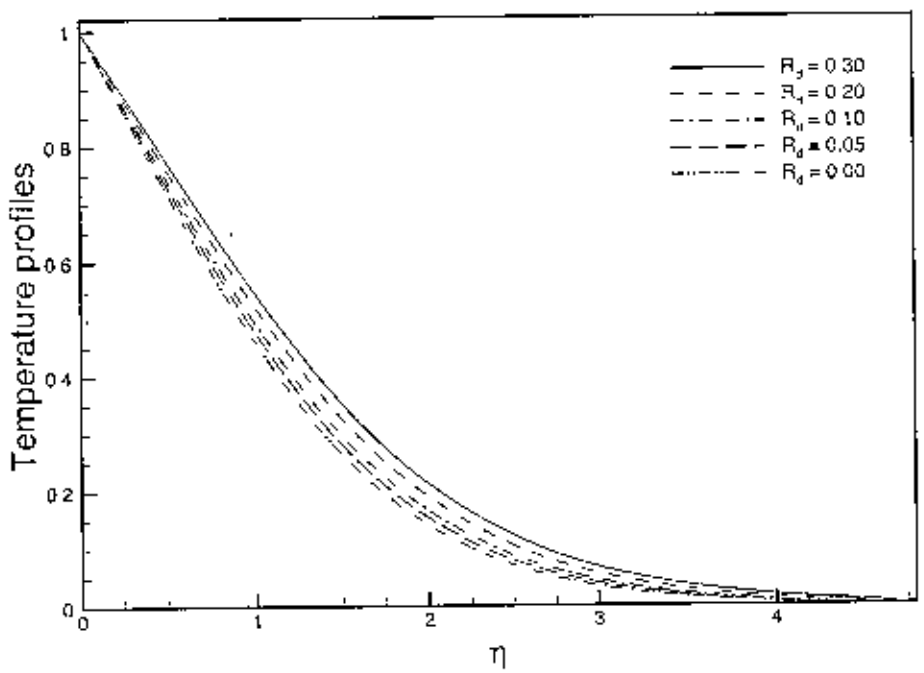

Figure 3.5: Temperature profiles for different values of Rd in case of Pr = 1.0, Q=2.0, θ_w = 1.1 and M.= 2.0

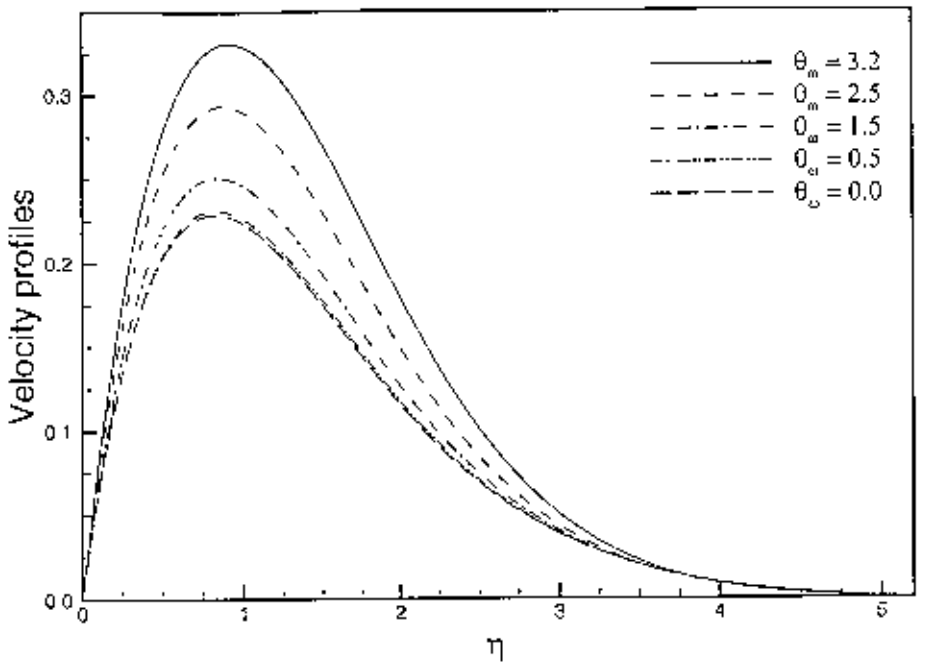

Figure 3.6: Velocity profiles for different values of θ_w in case of $Pr = 1.0$, $R_d = 0.1$, $Q = 2.0$ and $M = 2.0$

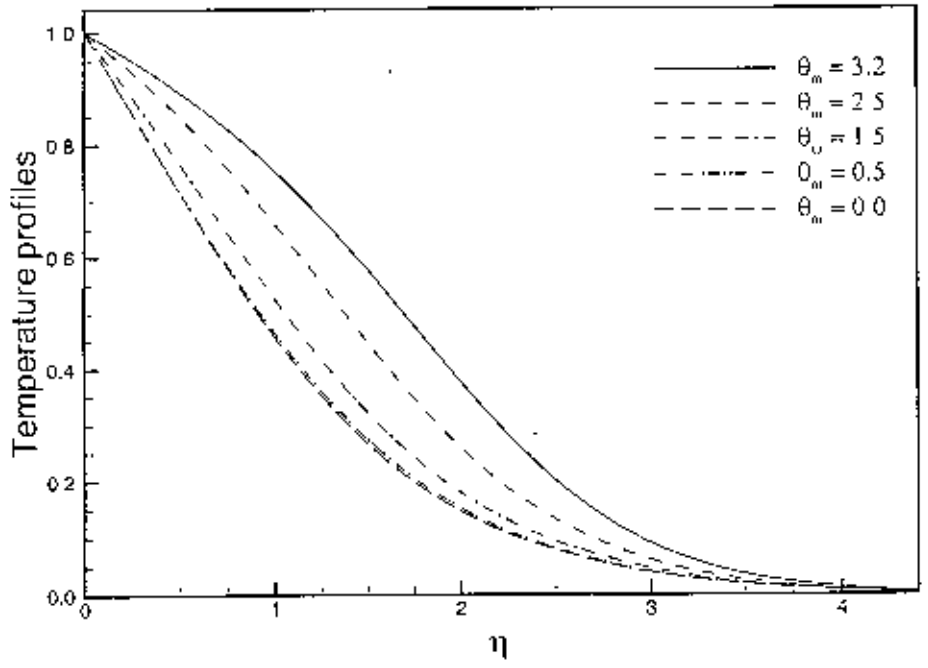

Figure 3.3: Temperature profiles for different values of θ_w in case of $Pr = 1.0$, $R_d = .1$, $Q = 2.0$ and M= 2.0

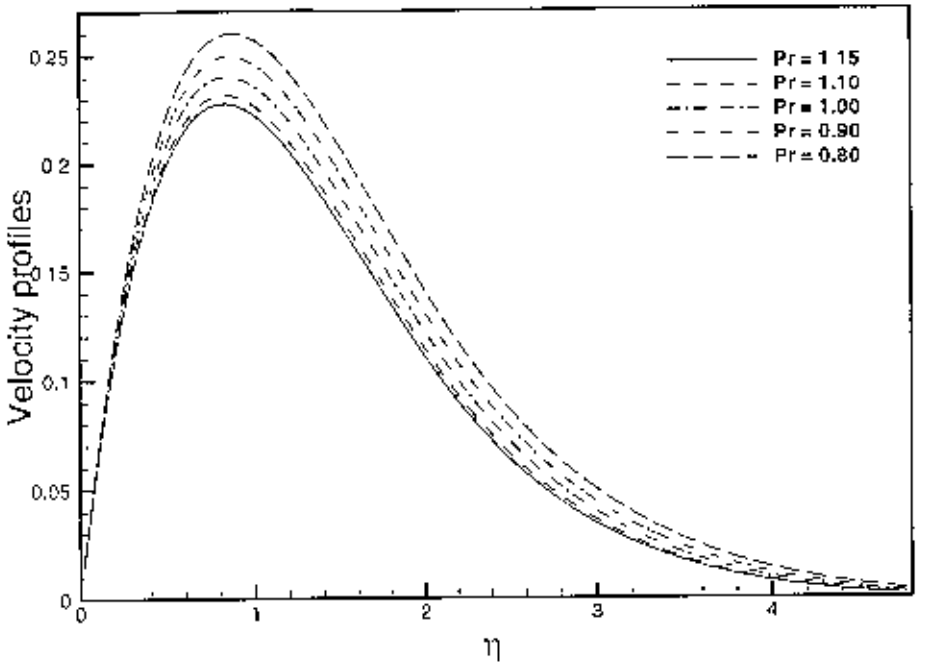

Figure 3.8: Velocity profiles for different values of Pr in case of R_d =.1, θv =1.1 , Q=2.0 and M= 2.0

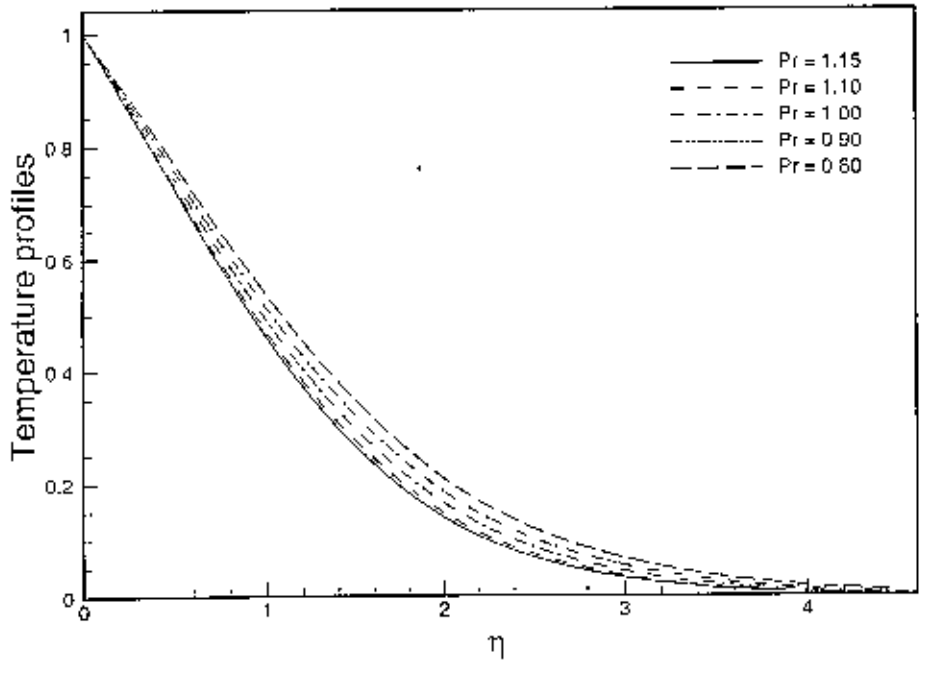

Figure 3.9: Temperature profiles for different values of Pr in case of R_d =0.1, θv =1.1, Q=2.0 and M= 2.0.

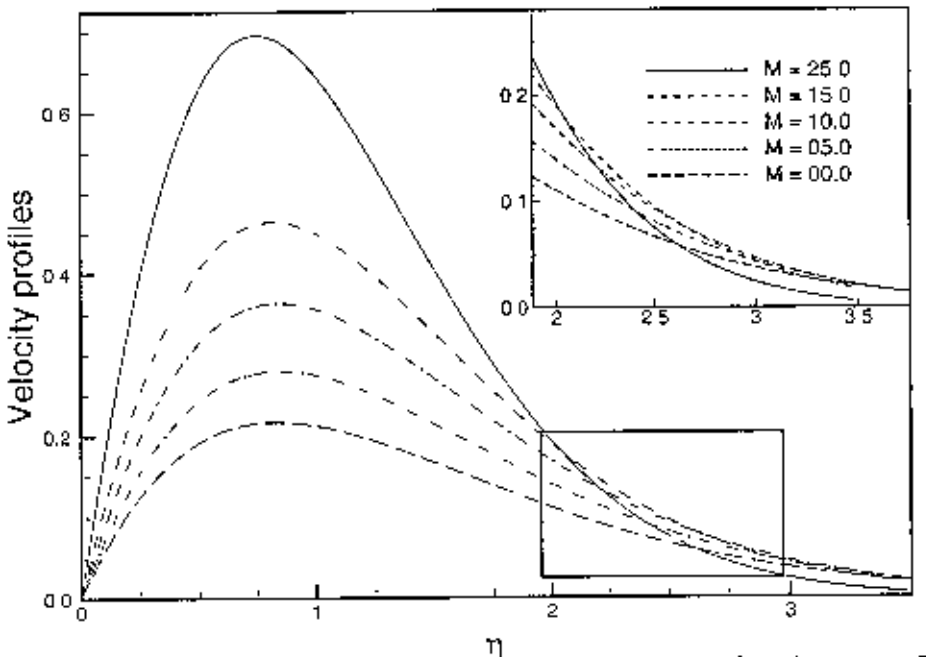

Figure 3.10: Velocity profiles for different values of M in case of R_d =0.1, θw =1.1, Q=2.0 and Pr=1.0

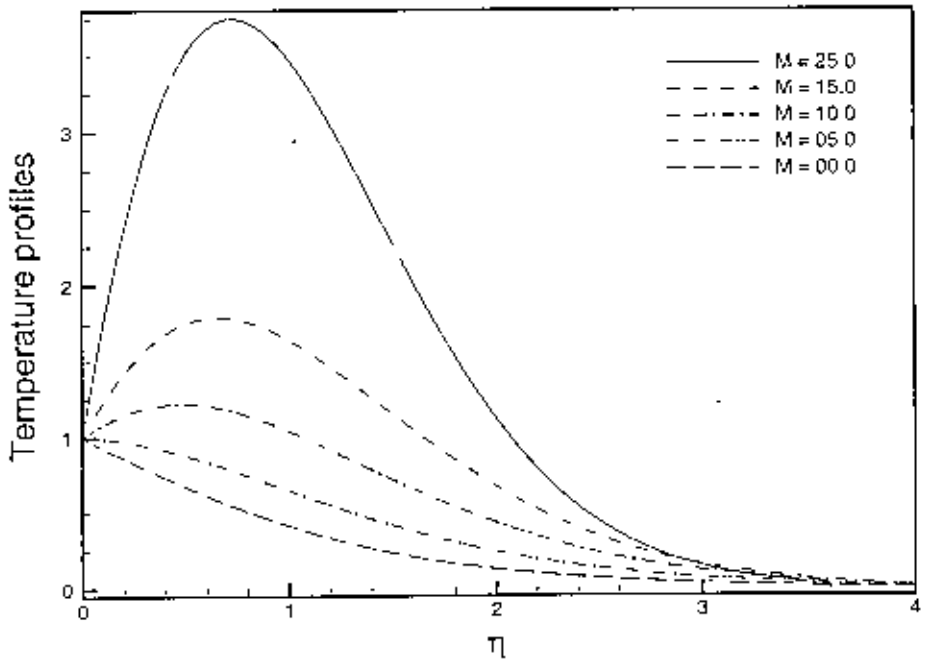

Figure 3.11: Temperature profiles for different values of M in case of R_d =0.1, θw =1.1, Q=2.0 and Pr=1.0

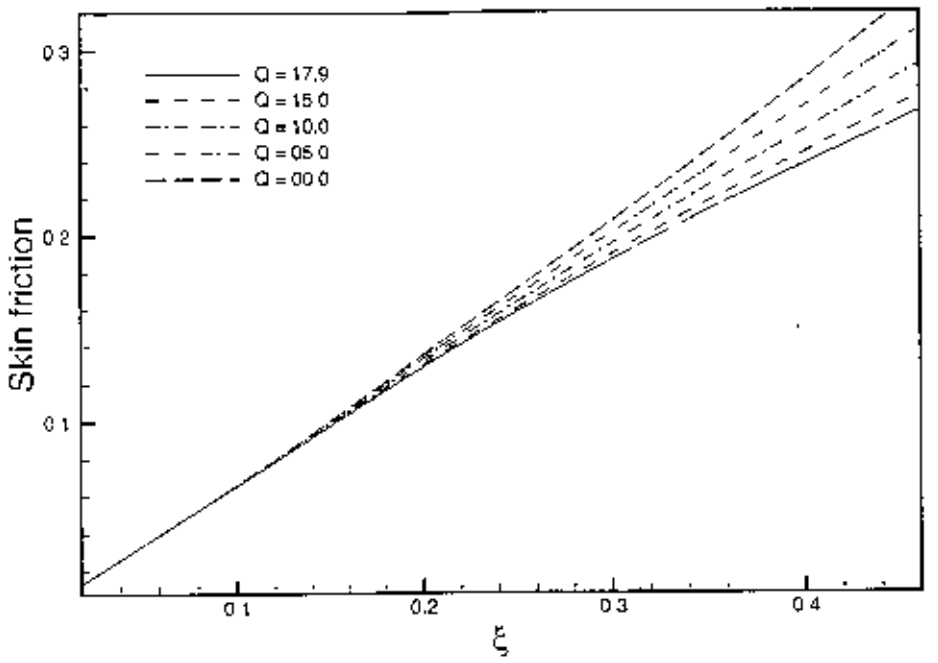

Figure 3.12: Skin-friction coefficient for different values of Q in case of Pr = 1.0, R_d =0.1, θw = 1.1 and M.= 2.0

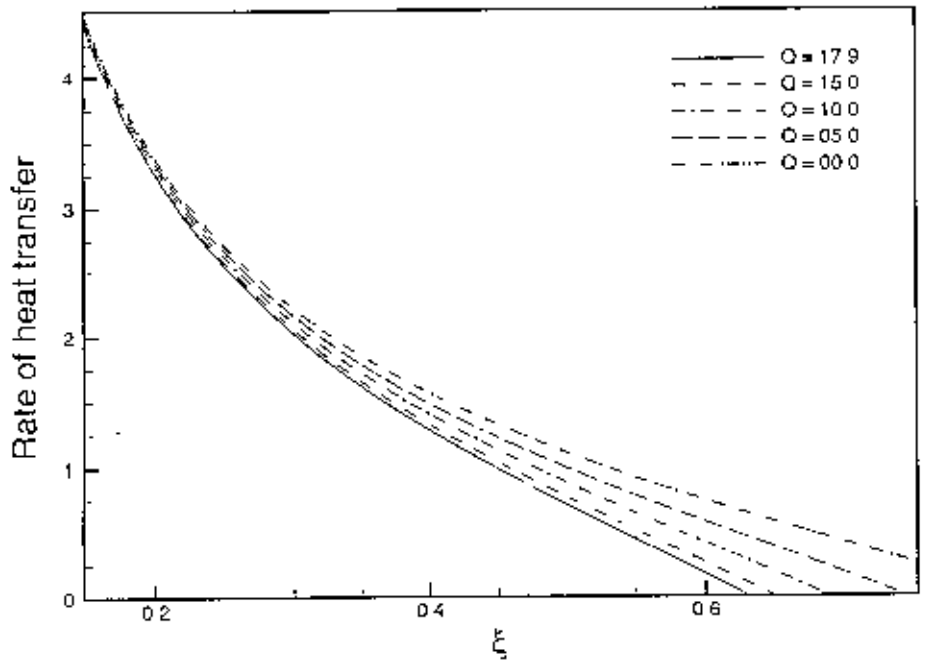

Figure 3.13: Rate of heat transfer for different values of Q in case of Pr = 1.0, R_d =0.1, θw = 1.1 and M.=2.0

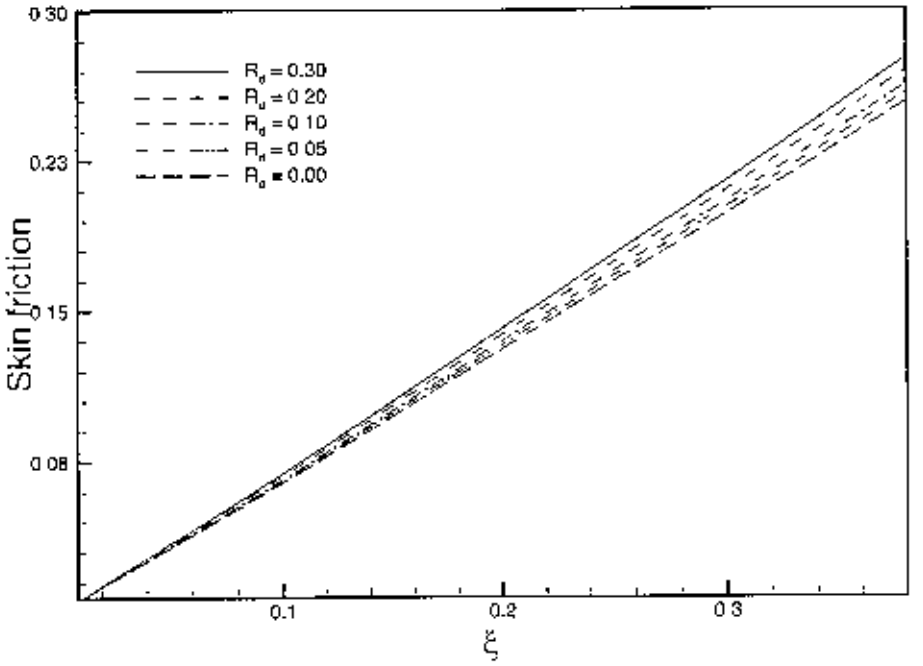

Figure 3.14: Skin-friction coefficient for different values of R_d in case of Pr = 1.0, θw =1.1, Q=2.0 and M=2. 0

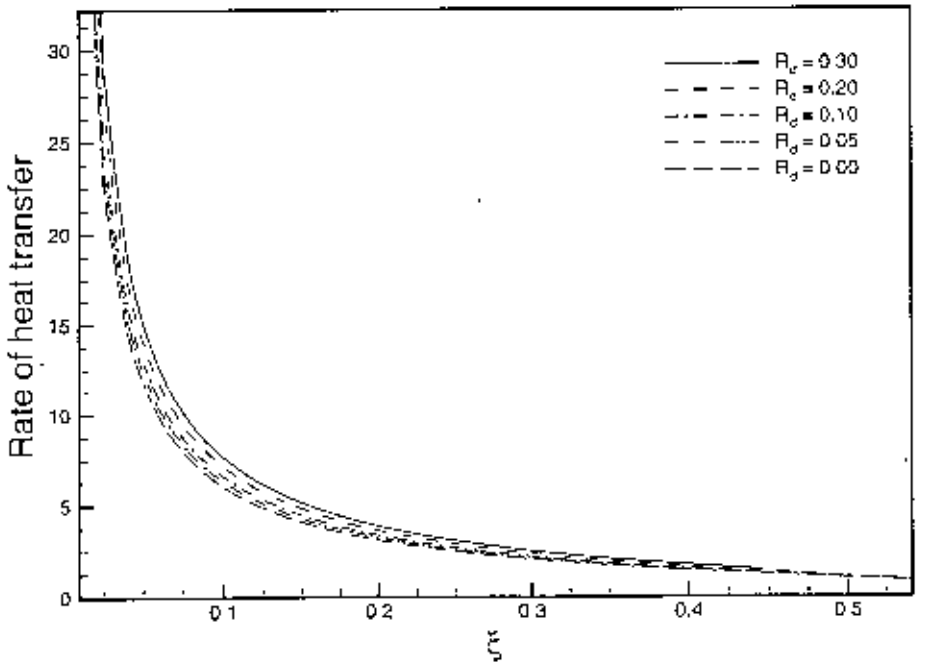

Figure 3.15: Rate of heat transfer for different values of R_d in case of Pr = 1.0, θw =1.1, Q=2.0 and M= 2.0

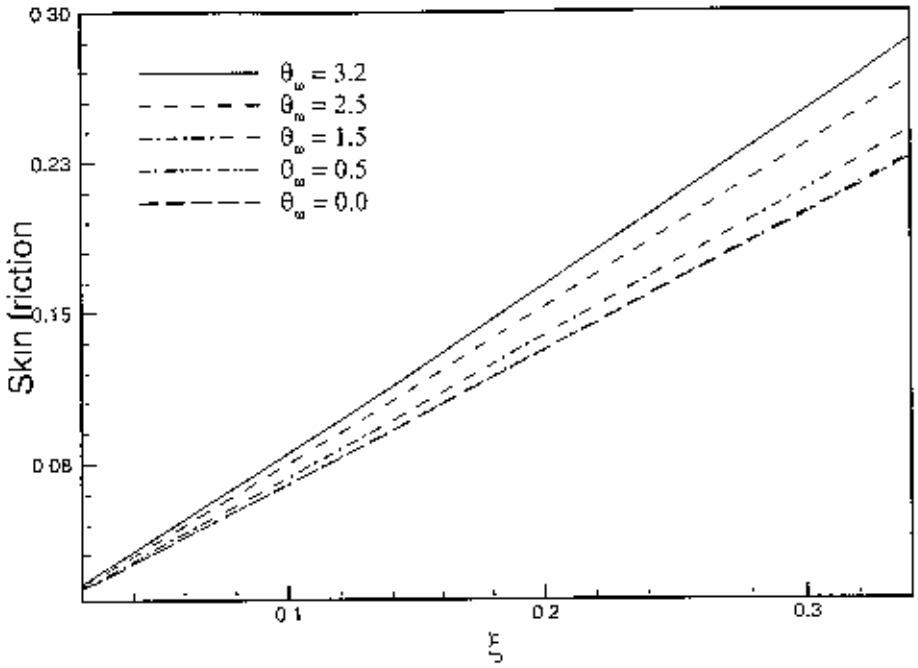

Figure 3.16: Skin-friction coefficient for different values of θw in case of Pr = 1.0, R_d =0.1 , Q=2.0 and M= 2.0

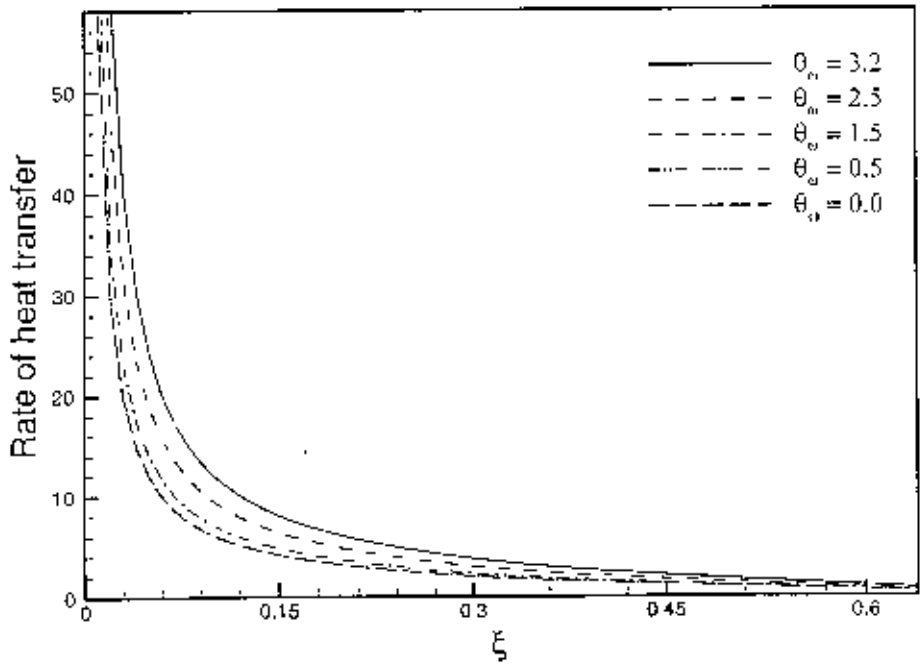

Figure 3.17: Rate of heat transfer for different values of θw in case of Pr = 1.0, R_d =0.1 , Q=2.0 and M=2.0

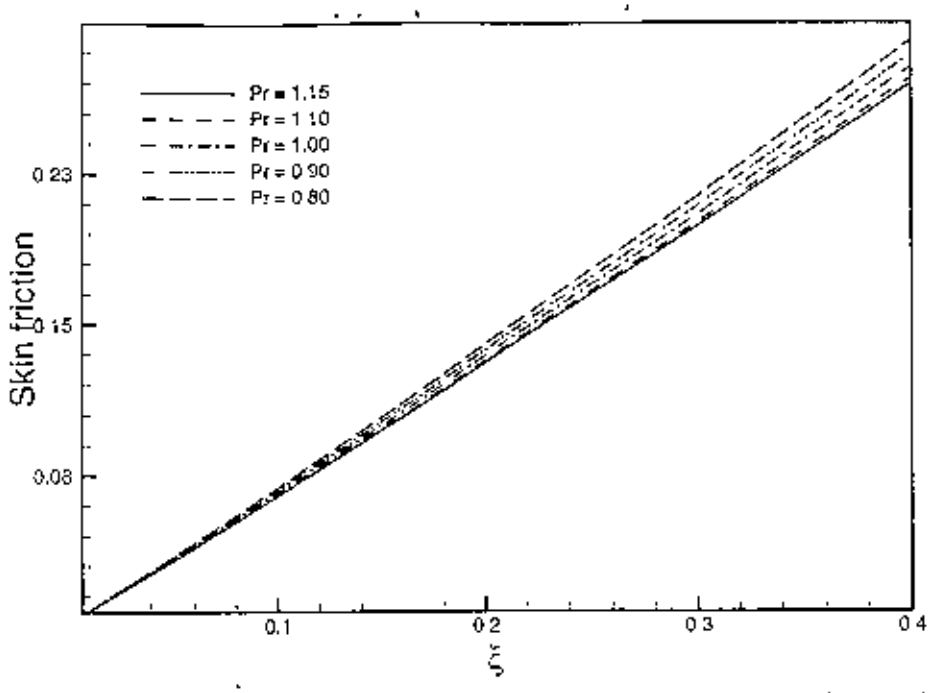

Figure 3.18: Skin-friction coefficient for different values of Pr while R_d =0.1, θw =1.1, Q=2.0 and M=2.0

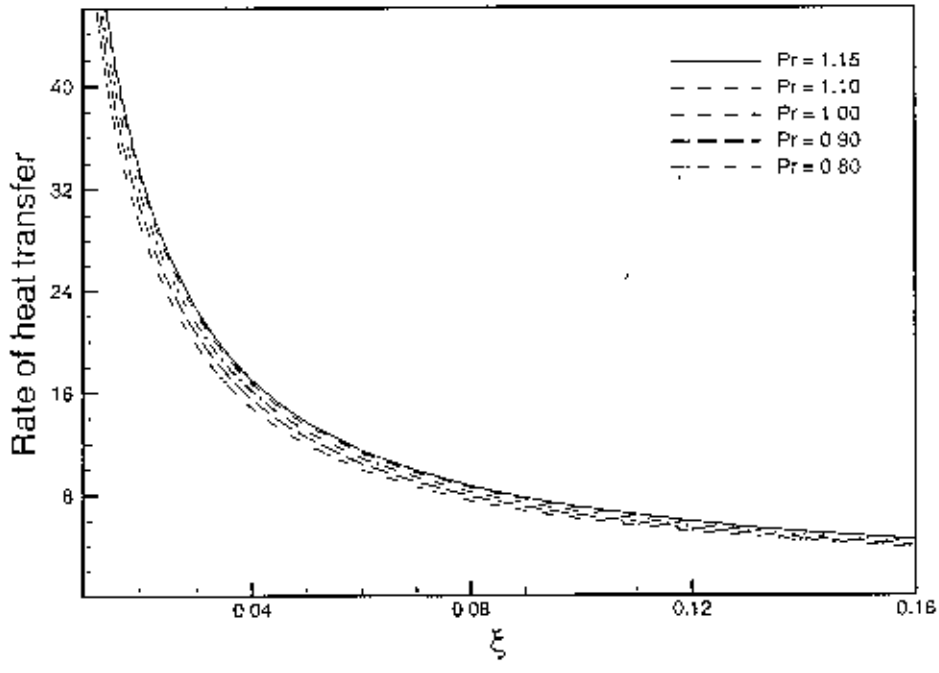

Figure 3.19: Rate of heat transfer for different values of Pr while R_d =0.1, θw =1.1, Q=2.0 and M=2 .0

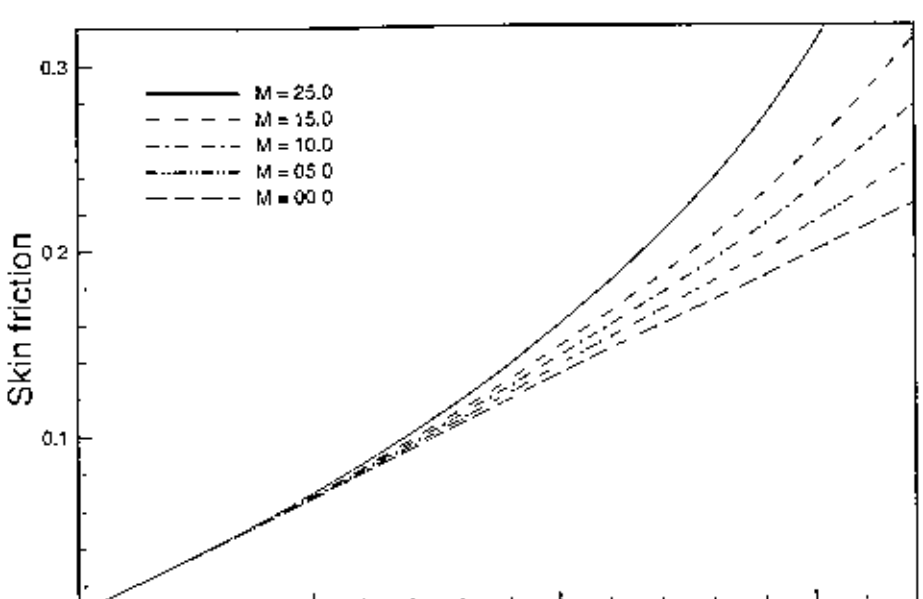

Figure 3.20: Skin-friction coefficient for different values of M in case of $Pr = 1.0$, R_d =0.1, θ_w =1.1 and Q=2.0

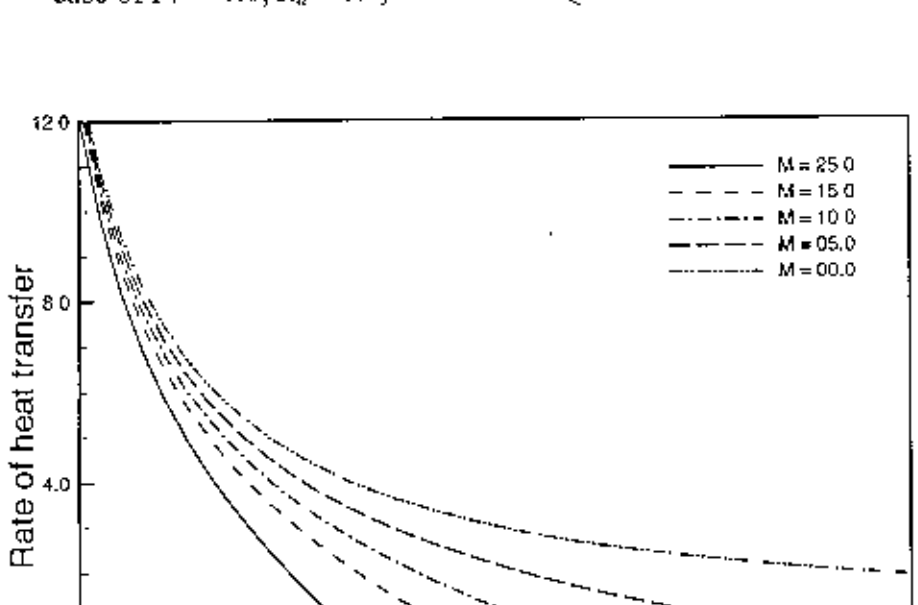

Figure 3.21: Rate of heat transfer for different values of M in case of $Pr = 1.0$, R_d =0.1, θ_w =1.1 and Q=2.0

3.4 Conclusion

For different values of relevant physical parameters including the magnetic parameter M, the effect of radiation on natural convection flow from a porous vertical plate in presence of heat generation has been investigated. The governing boundary layer equations of motion are transformed into a non-dimensional form and the resulting non-linear systems of partial differential equations are reduced to local non-similarity boundary layer equations, which are solved numerically by using implicit finite difference method together with the Keller-box scheme. From the present investigation the following conclusions may be drawn:

- Significant effects of heat generation parameter Q and magnetic parameter M on velocity and temperature profiles as well as on skin friction coefficient C_f, and the rate of heat transfer Nu_x have been found in this investigation but the effect of heat generation parameter Q and magnetic parameter M on rate of heat transfer is more significant. An increase in the values of heat generation parameter Q leads to the velocity decrease and the temperature profiles increase, the local skin friction coefficient C_{fx} and the local rate of heat transfer Nu_x decreases at different position of ξ for Pr =1.0
- All the velocity profile, temperature profile and the local skin friction coefficient C_{fx} and the local rate of heat transfer Nu_x significantly increase when the values of radiation parameter R_d increase
- As surface temperature parameter θ_w increases, both the velocity and the temperature profile increase and also the local rate of heat transfer Nu_x and the local skin friction coefficient C_{fx} significantly increases
- For increasing values of Prandtl number Pr leads to decrease the velocity profile, the temperature profile and the local skin friction coefficient C_{fx} but the local rate of heat transfer Nu_x increases.
- An increase in the values of M leads to increase the velocity profiles and the temperature profiles and also the local skin friction coefficient C_{fx} increase but and the local rate of heat transfer Nu_x decreases.

3.5 Comparison of the results

Figure 3.22 depicts the comparisons of the present numerical results of the Nusselt number Nu with Hossain et al. (1998). Here, the radiation, heat generation and magnetic effects are ignored (i.e., R_d =0.05, Q =0.0 and M =0.0) and Prandtl numbers Pr =1.0 and θ_w =1.1, θ_w =1.5, θ_w =2.5 are chosen. In this work the results helped me to take firm decision that the

present results agreed well with the solutions of Hossain et al. (1998) in the presence of suction.

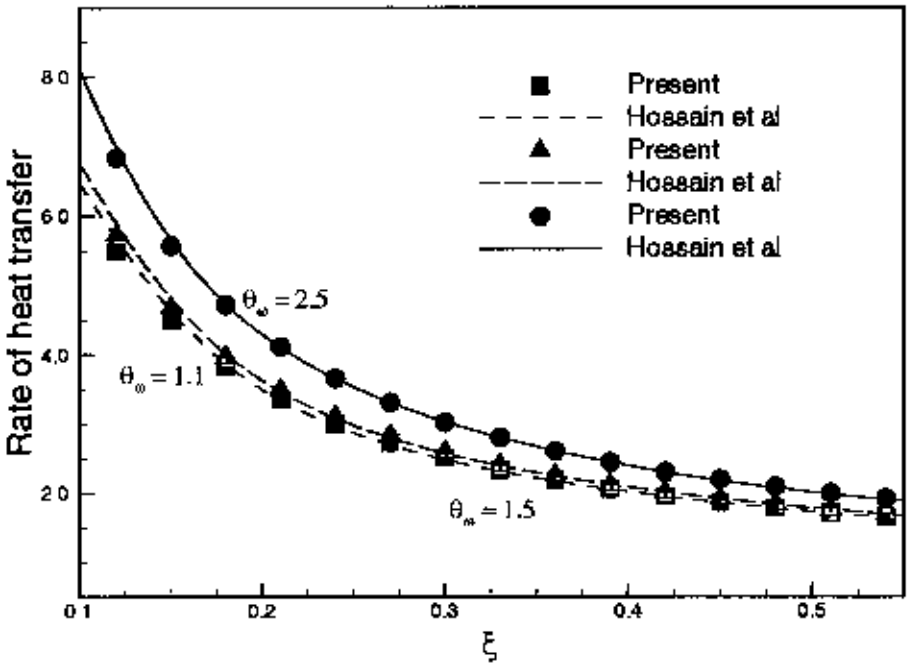

Figure 3.22: Comparisons of the present numerical results of Nusselt number Nu for the Prandtl numbers Pr =1.0 with those obtained by Hossain et al (1998).

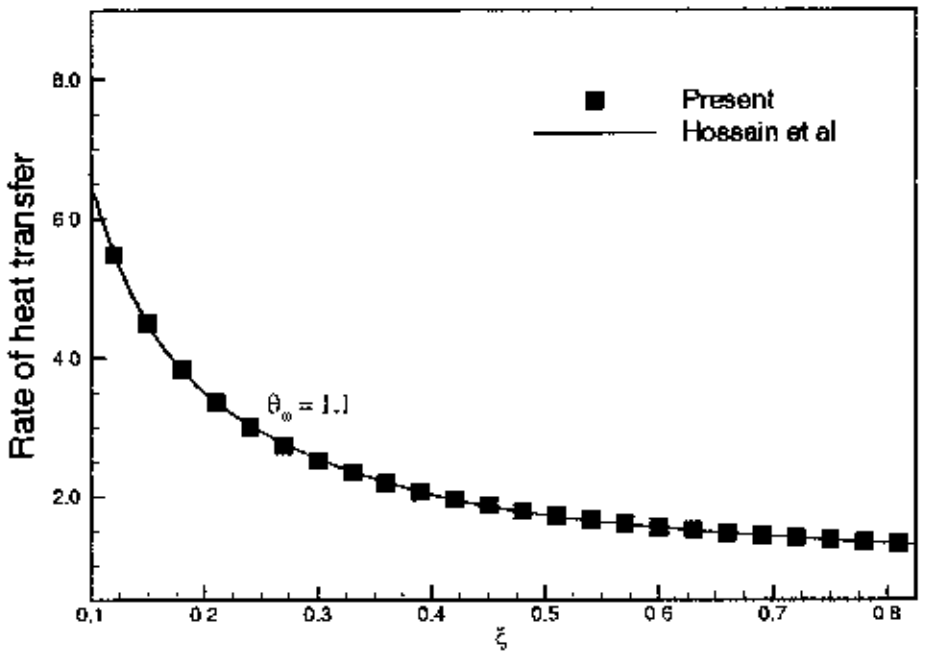

Figure 3.22(a): Comparisons of the present numerical results of Nusselt number Nu for the Prandtl numbers Pr =1.0 and θ_w =1.1 with those obtained by Hossain et al. (1998).

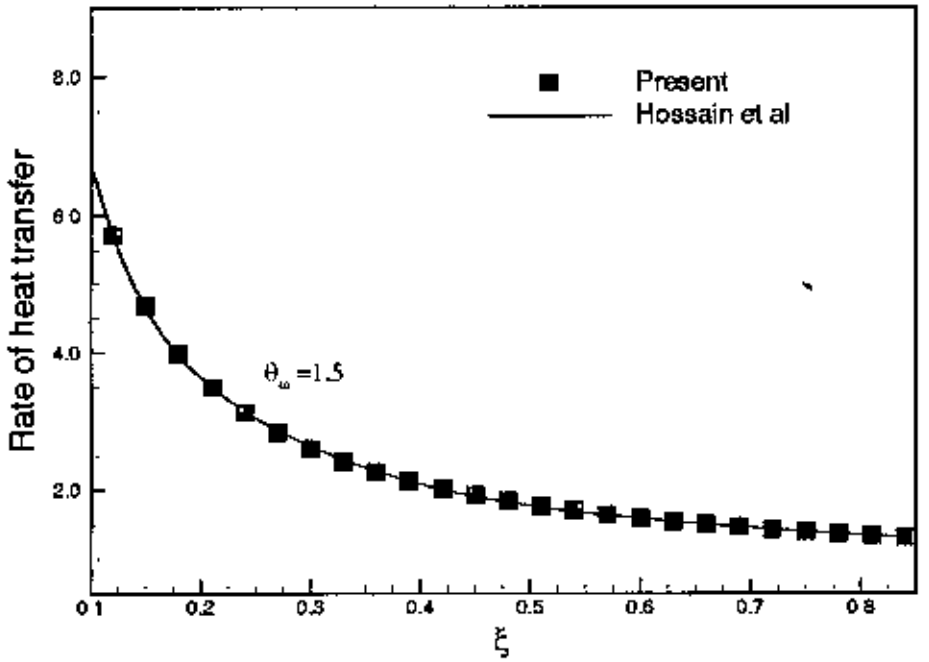

Figure 3.22(b): Comparisons of the present numerical results of Nusselt number Nu for the Prandtl numbers Pr =1.0 and θ_w=1.5 with those obtained by Hossain et al. (1998).

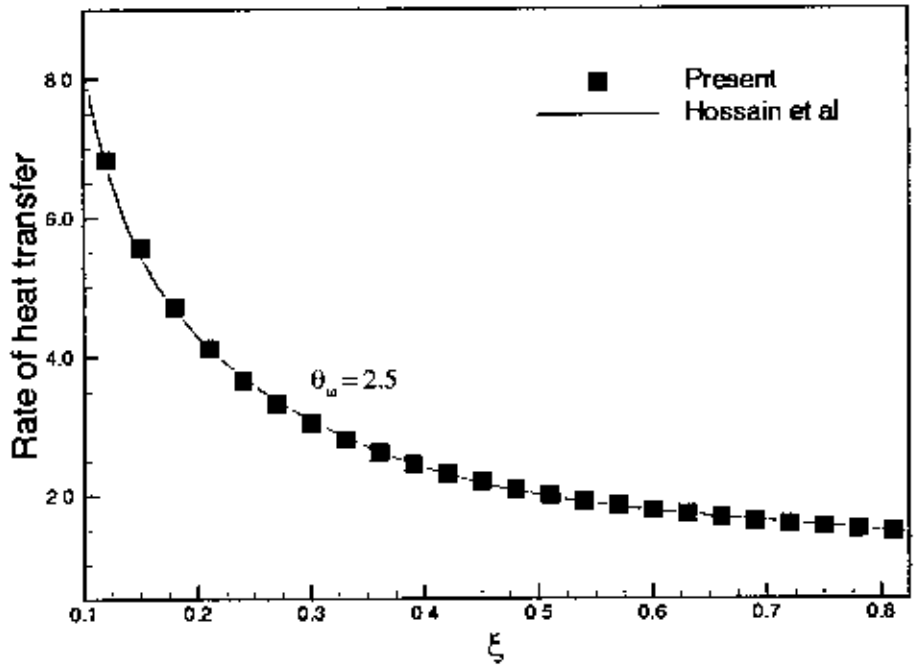

Figure 3.22(c): Comparisons of the present numerical results of Nusselt number Nu for the Prandtl numbers Pr =1.0 and θ_w=2.5 with those obtained by Hossain et al (1998).

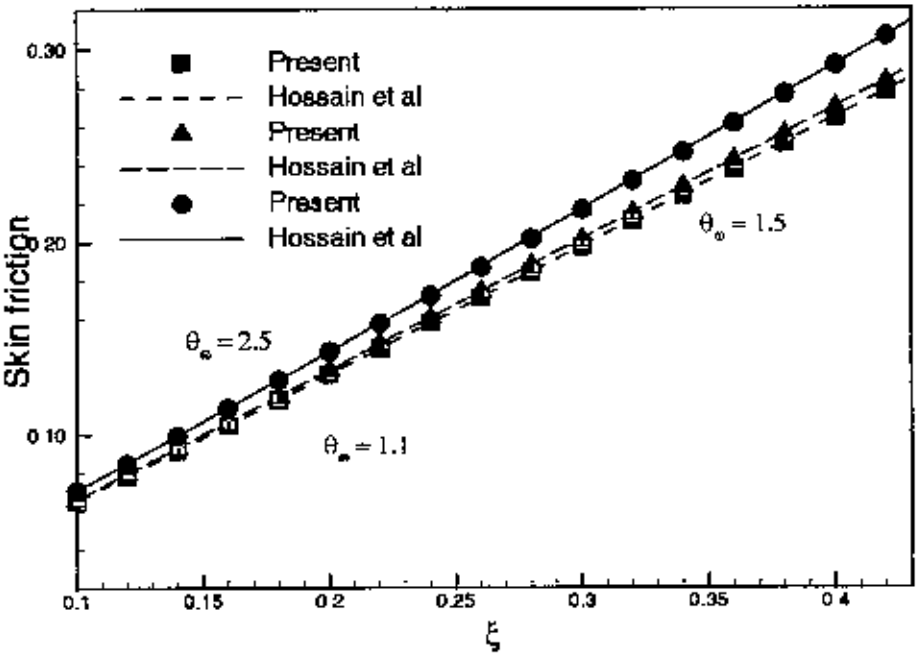

Figure 3.23: Comparisons of the present numerical results of Skin friction coefficient C_{fx} for the heat generation parameter θ_w = 1.1, 1.5 and 2.5 with those obtained by Hossain et al (1998).

Figure 3.23 shows the comparisons of the present numerical results of the skin friction coefficients C_{fx} with Hossain et al (1998) for different values of surface temperature which are θ = 1.1, 1.5 and 2.5. Here, the radiation and the magnetic effects are ignored (i.e., R_d

=0.0 and M =0.0) and Prandtl numbers Pr = 1 0 have been chosen The comparison shows fairly good agreement between the present results and the results of Hossain et al (1998).

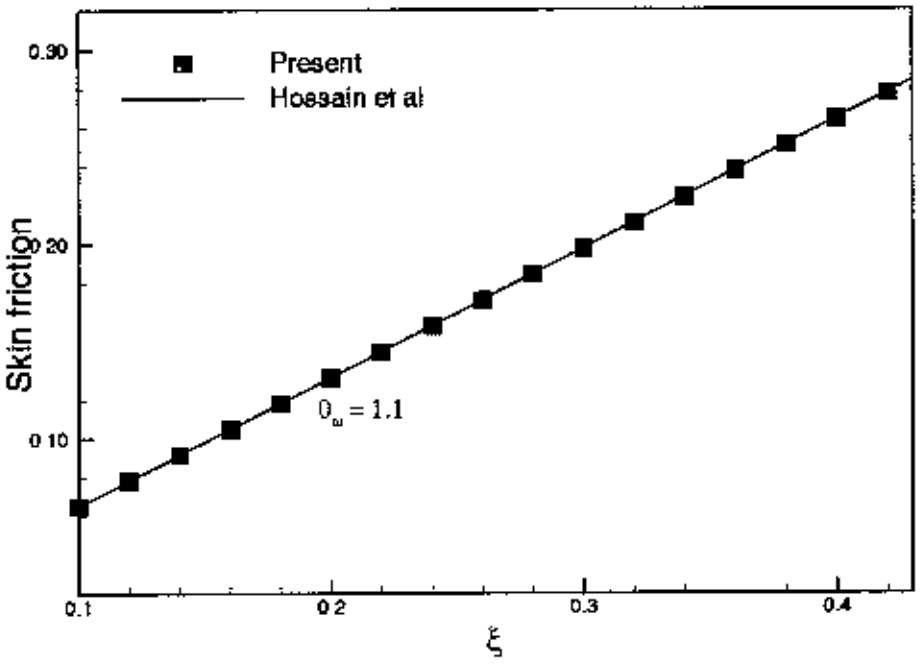

Figure 3.23(a): Comparisons of the present numerical results of Skin friction coefficient C_{fx} for the heat generation parameter θ_w = 1.1 with those obtained by Hossain et al (1998).

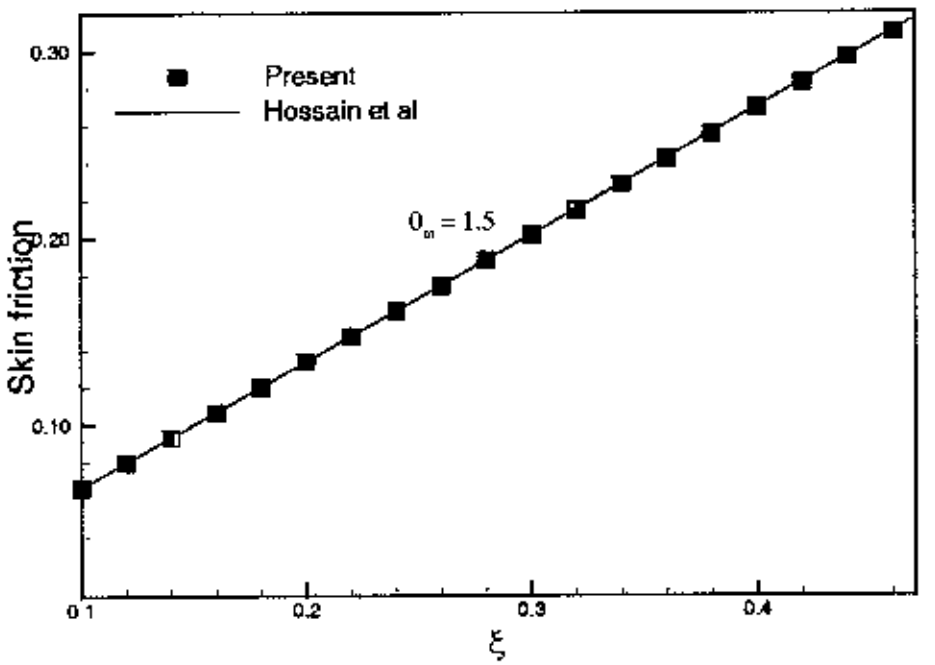

Figure 3.23(b): Comparisons of the present numerical results of Skin friction coefficient C_{fx} for the heat generation parameter $\theta_w = 1.5$ with those obtained by Hossain et al (1998)

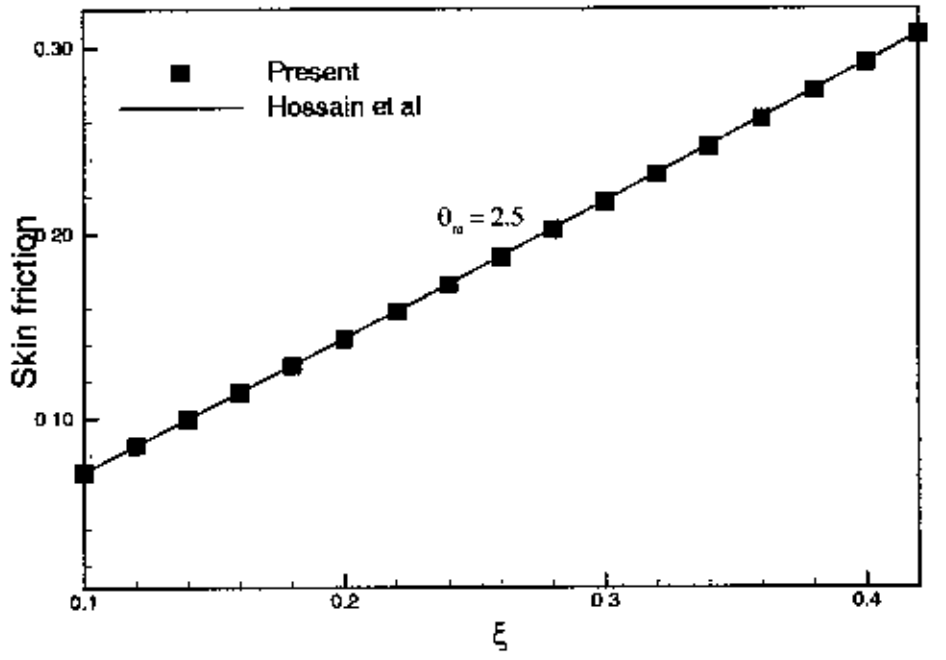

Figure 3.23(c): Comparisons of the present numerical results of Skin friction coefficient C_{fx} for the heat generation parameter $\theta_w = 2.5$ with those obtained by Hossain et al (1998)

3.6 Extension of this work

In this work, we considered constant viscosity and thermal conductivity but they are functions of temperature.

- If we consider the viscosity and thermal conductivity as the function of temperature then we can extend our problem.
- Also taking the non-uniform surface temperature, the problem can be extended.

References

[1] M. A Hossain, M. A. Alim, D. A. S. Rees, The effect of radiation on free convection flow from a porous vertical plate, International Journal of Heat and Mass Transfer, Vol. 42, pp. 81-91, (1999).

[2] V. M. Soundalgekar, H.S. Takhar N.V. Vighnesam, The combined free and forced convection flow past a semi infinite vertical plate with variable surface temperature, Nuclear Engineering and Design, Vol. 110, pp. 95-98, (1960).

[3] M A. Hosain, H.S. Takhar, Radiation effect on mixed convection along a vertical plate with uniform surface, Temperature, Heat and Mass Transfer, Vol. 31, pp. 243-248, (1996).

[4] E. M. Sparrow, R.D. Cess, Free convection with blowing or suction, Journal of heat transfer, Vol. 83, pp. 387-396, (1961).

[5] J. H. Merkin, Free convection with blowing and suction, International journal of heat and mass transfer, Vol. 15. pp. 989-999, (1972).

[6] M.M. Molla, M.A. Hossain, L.S. Yao, Natural convection flow along a vertical wavy surface with uniform surface temperature in presence of heat generation/absorption, International Journal of Thermal Science Vol 43, pp. 157–163. (2004).

[7] Md. Miraj Ali, "Numerical Study of Radiation on Natural Convection Flow on a Sphere with Heat Generation", M.Phil Thesis, Department of Mathematics, Bangladesh University of Engineering and Technology (BUET), Dhaka, Bangladesh, (2007).

[8] Tahmina Akhter, "Effect of Radiation on Natural Convection Flow on a Sphere with Isothermal surface and uniform Heat Flux", M.Phil Thesis. Department of Mathematics, Bangladesh University of Engineering and Technology (BUET), Dhaka, Bangladesh, (2007).

[9] A.C Cogley, W.G Vincenti, S.E. Giles, Differential approximation for radiative in a non-gray gas near equilibrium, AIAA Journal, Vol. 6.pp. 551-553(1968).

[10] R. Eichhorn, The effect of mass transfer on free convection, Journal of Heat Transfer, Vol. 82, pp. 260-263, (1960).

[11] J.F. Clarke, Transpiration and natural convection: the vertical flat plate problem, Journal of Fluid Mechanics, Vol. 57, pp. 45-61, (1973).

[12] H.J. Merkin, The effects of blowing and suction on free convection boundary layers, International Journal of Heat and Mass Transfer. Vol. 18, pp. 237-244, (1975).

[13] M. Vedhanayagam, R.A. Altenkirch, R. Eichhorn, A transformation of the boundary layer equations for free convection past a vertical flat plate with arbitrary blowing and wall temperature variations, International Journal of Heat and Mass Transfer, Vol. 23, pp. 1286-1288, (1980).

[14] J.F Clarke, N. Riley, Natural convection induced in a gas by the presence of a hot porous horizontal surface. Q.J. Mech. Appl. Math., Vol. 28, pp. 373-396. (1975).

[15] J.F. Clarke, N. Riley, Free convection and the burning of a horizontal fuel surface, Journal of Fluid Mechanic, Vol. 74, pp. 415-431, (1976).

[16] H T. Lin, W. S. Yu, Free convection on a horizontal plate with blowing and suction, Transactions of ASME Journal of Heat Transfer, Vol. 110, pp 793-796. (1988).

[17] H.B. Keller, Numerical methods in boundary layer theory, Annual Review of Fluid Mechanics, Vol. 10, pp. 417-433, (1978).

[18] M. M. Ali, T.S. Chen, B. F. Armaly, Natural convection- radiation interaction in boundary layer flow over horizontal surfaces, AIAA Journal, Vol. 22, pp. 1797-1803, (1984).

[19] R. Siegel, J.R. Howell, Thermal Radiation Heat Transfer, McGraw Hill, New York, (1972).

[20] E.M. Sparrow, H.S. Yu, Local non similarity thermal boundary layer solutions, Transactions of ASME Journal of Heat Transfer, Vol. 93, pp. 328-334, (1971).

[21] T.S Chen, Parabolic systems: local non-similarity method, in: W.J. Minkowycz, (Ed) Hand book of Numerical Heat Transfer , Wiley, New York, Chapter 5, (1988).

[22] M.A Hossain, N. Banu, A. Nakayama, Non-Darcy forced convection boundary layer flow over a wedge embedded in a saturated porous medium. Numerical Heat Transfer Part A, Vol. 26, pp. 399-414, (1994).

[23] T. Cebeci, P. Bradshaw, Physical and Computational Aspects of Convective Heat Transfer, Springer, New York,(1984).

[24] M.A. Hossain, Effect of transpiration on combined heat and mass transfer in mixed convection along a vertical plate, International Journal of Energy Research, Vol 17, pp. 761-769, (1992).

[25] J C. Butcher, Implicit Runge-Kutta processes, Math. Comp. 18(1964), 50-55.

[26] P.R. Nachtsheim, P.Swigert, Satisfaction of asymptotic boundary conditions in numerical solution of systems of non-linear equation of boundary layer type. NASATND, 3004, (1965).

[27] T.Y. Na, Computational Method in Engineering Boundary Value Problems, Academic Press, New York, (1979).

[28] M.N. Ozisik, Radiative Transfer and Interactions with Conduction and Convection, Wiley, New York, (1987).

[29] Md. Mamun Molla, Md. Anwar Hossain, Md, Abu Taher, Magnetohydrodynamic natural convection flow on a spere with uniform heat flux in presence of heat generation. Acta Mechanica Vol. 186, pp. 75-86. (2006).

[30] Radiative heat transfer,.Michael E. Modest, McGraw –Hill, NewYork.

[31] K. Vejravelu. A. Hadjinicolaou, Heat transfer in a viscous fluid over a stretching sheet with viscous dissipation and internal heat generation. Int. comm. Heat Transfer, Vol. 20, pp. 417-430, (1993).

[32] Wikipedia online encyclopedia, http://en.wikipedia org/Magnetohydrodynamic, (2009).

[33] Wikipedia online encyclopedia, http://en.wikipedia.org/wiki/Heat_equation, (2009).

Appendix

Implicit Finite Difference Method

Implicit finite difference method in conjunction with Keller- box elimination technique is engaged to dig up the solutions of the transformed governing equations with the corresponding boundary conditions. This practice is well documented and widely used by Keller and Cebeci (1971) and recently by Hossain et al. (1990, 1992, 1996, 1997, and 1998).

Accompanied by Keller –box elimination scheme, an epigrammatic discussion on the advancement of algorithm on implicit finite difference method is given below taking into account the following Equations (1-2).

$$f''' + 3ff'' - 2(f')^2 + \theta - \xi f'' - Mf'\xi^2 = \xi\left(f'\frac{\partial f'}{\partial \xi} - \frac{\partial f}{\partial \xi}f''\right) \tag{1}$$

And

$$\frac{1}{\Pr}\frac{\partial}{\partial \eta}\left[\left\{1+\frac{4}{3}Rd\left(1+(\theta_w-1)\theta\right)^3\right\}\frac{\partial \theta}{\partial \eta}\right] + Q\theta + 3f\theta' + \xi\theta' = \xi\left(f'\frac{\partial \theta}{\partial \xi} - \frac{\partial f}{\partial \xi}\theta'\right) \tag{2}$$

To apply the aforementioned method, we first convert Equations (1)-(2) into the following system of first order equations with dependent variables $u(\xi,\eta)$, $v(\xi,\eta)$, $p(\xi,\eta)$ and $g(\xi,\eta)$ as

$$f' = u,\ u' = v,\ \ g = \theta,\ \text{and}\ \ \theta' = p \tag{3}$$

$$v' + p_1 fv - p_2 u^2 + g - \xi v - p_5 u\xi^2 = \xi\left(u\frac{\partial u}{\partial \xi} - \frac{\partial f}{\partial \xi}v\right) \tag{4}$$

$$\Rightarrow \frac{1}{\Pr}\frac{\partial}{\partial \eta}\left[\left\{1+p_3\left(1+\Delta g\right)^3\right\}p\right] + p_4 g + \xi p + p_1 fp = \xi\left(u\frac{\partial g}{\partial \xi} - p\frac{\partial f}{\partial \xi}\right)$$

$$\Rightarrow \frac{1}{\Pr}\left[p' + \left|\{p_3 p(1+\Delta g)\}'\right|^3\right] + p_4 g + \xi p + p_1 fp = \xi\left(u\frac{\partial g}{\partial \xi} - p\frac{\partial f}{\partial \xi}\right) \tag{5}$$

where

$$p_1 = 3,\ p_2 = 2,\ p_3 = \frac{4}{3}Rd\ ,\ p_4 = Q,\ p_5 = M \tag{6}$$

The corresponding boundary conditions are

$$\begin{aligned} &f(\xi,0) = 0, u(\xi,0) = 0 and g(\xi,0) = 0 \\ &u(\xi,\infty) = 0, g(\xi,\infty) = 0 \end{aligned} \tag{7}$$

We now consider the net rectangle on the (ξ,η) plane and denote the net point by

$$\eta_0 = 0,\quad \eta_j = \eta_{j-1} + h_j,\qquad j = 1,2,\ldots J$$

$$\xi^0 = 0\ ,\quad \xi^n = \xi^{n-1} + k_n\ ,\quad n = 1,2,\ldots\ N$$

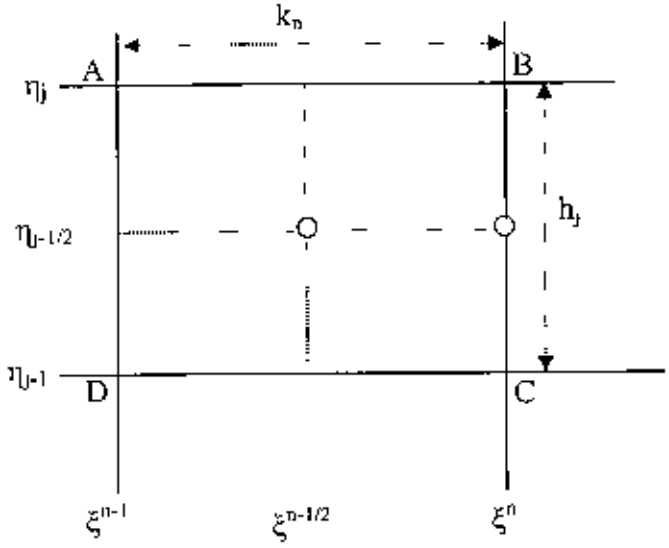

Figure A1: Net rectangle for difference approximations for the Box scheme

Here 'n' and 'j' are just sequence of numbers on the (ξ,η) plane, k_n and h_j are the variable mesh widths.

We approximate the quantities $(f,\ u,\ v,\ p)$ at the points (ξ^n,η_j) of the net by $(f_j^n,u_j^n,v_j^n,p_j^n)$ which we call net function. We also employ the notation g_j^n for the quantities midway between net points shown in Figure (A1) and for any net function as

$$\xi^{n-1/2} = \frac{1}{2}(\xi^n + \xi^{n-1}) \tag{8}$$

$$\eta_{j-1/2} = \tfrac{1}{2}(\eta_j - \eta_{j-1})$$

$$g_j^{n-1/2} = \tfrac{1}{2}(g_j^n + g_j^{n-1})$$

$$g_{j-1/2}^n = \tfrac{1}{2}(g_j^n + g_{j-1}^n)$$

Now we write the difference equations that are to approximate Equations (3) - (5) by considering one mesh rectangle for the mid point $(\xi^n, n_{j-1/2})$ to obtain

$$\frac{f_j^n - f_{j-1}^n}{h_j} = u_{j-1/2}^n \tag{9}$$

$$\frac{u_j^n - u_{j-1}^n}{h_j} = v_{j-1/2}^n \tag{10}$$

$$\frac{g_j^n - g_{j-1}^n}{h_j} = p_{j-1/2}^n \tag{11}$$

$$\frac{1}{2}\left(\frac{v_j^n - v_{j-1}^n}{h_j} + \frac{v_j^{n-1} - v_{j-1}^{n-1}}{h_j}\right) + (p_1 fv)_{j-\frac{1}{2}}^{n-\frac{1}{2}} - (p_2 u^2)_{j-\frac{1}{2}}^{n-\frac{1}{2}} + (g)_{j-\frac{1}{2}}^{n-\frac{1}{2}} - (\xi v)_{j-\frac{1}{2}}^{n-\frac{1}{2}} - (p_3 u \xi^2)_{j-\frac{1}{2}}^{n-\frac{1}{2}}$$
$$= (\xi)_{j-\frac{1}{2}}^{n-\frac{1}{2}}\left((u)_{j-\frac{1}{2}}^{n-\frac{1}{2}} \frac{u_j^n - u_{j-1}^n}{k_n} + (v)_{j-\frac{1}{2}}^{n-\frac{1}{2}} \frac{f_j^{n-1} - f_{j-1}^{n-1}}{k_n}\right)$$

$$\frac{1}{\mathrm{Pr}}\left[\frac{h_j^{-1}}{2}[(p_j^n - p_{j-1}^n) + (p_j^{n-1} - p_{j-1}^{n-1})] + \frac{h_j^{-1}}{2}[(\{p_3 p(1+\Delta g)^3\}_j^n - \{p_3 p(1+\Delta g)^3\}_{j-1}^n) + (\{p_3 p(1+\Delta g)^3\}_j^{n-1} - \{p_3 p(1+\Delta g)^3\}_{j-1}^{n-1})]\right]$$
$$+ (p_4 g)_{j-1/2}^{n-1/2} + (p_1 f p)_{j-1/2}^{n-1/2} + (\xi p)_{j-1/2}^{n-1/2}$$
$$= \xi_{j-1/2}^{n-1/2}\left\{u_{j-1/2}^{n-1/2}\left(\frac{g_{j-1/2}^n - g_{j-1/2}^{n-1}}{k_n}\right) + p_{j-1/2}^{n-1/2}\left(\frac{f_{j-1/2}^n - f_{j-1/2}^{n-1}}{k_n}\right)\right\}$$

Similarly equations (4) – (5) are approximate by centering about the mid point $(\xi^{n-1/2}, n_{j-1/2})$. Centering the equations (8) about the point $(\xi^{n-1/2}, n)$ without

specifying η to obtain the algebraic equations. The difference approximation to Equations (4)-(5) become

$$h_j^{-1}(v_j^n - v_{j-1}^n) + \{(p_1)_{j-1/2}^n + \alpha_n\}(fv)_{j-1/2}^n - \{(p_2)_{j-1/2}^n + \alpha_n\}(u^2)_{j-1/2}^n + g_{j-1/2}^n$$
$$-(\xi v)_{j-1/2}^n + \alpha_n\{f_{j-1/2}^n v_{j-1/2}^{n-1} - v_{j-1/2}^n f_{j-1/2}^{n-1}\} - (p_5)_{j-1/2}^n u_{j-1/2}^n (\xi^2)_{j-1/2}^n = R_{j-1/2}^{n-1}$$

Where

$$L_{j-\frac{1}{2}}^{n-1} = (p_1)_{j-\frac{1}{2}}^{n-1}(fv)_{j-\frac{1}{2}}^{n-1} - (p_2)_{j-\frac{1}{2}}^{n-1}(u^2)_{j-\frac{1}{2}}^{n-1} + g_{j-\frac{1}{2}}^{n-1}$$
$$-(\xi p)_{j-\frac{1}{2}}^{n-1} + h_j^{-1}(v_j^{n-1} - v_{j-1}^{n-1}) - (p_5)_{j-1/2}^{n-1} u_{j-1/2}^{n-1}(\xi^2)_{j-1/2}^{n-1}$$

and $R_{j-\frac{1}{2}}^{n-1} = -L_{j-\frac{1}{2}}^{n-1} + \alpha_n\left\{-(u^2)_{j-\frac{1}{2}}^{n-1} + (fv)_{j-\frac{1}{2}}^{n-1}\right\}$

$$\frac{1}{\Pr}[h_j^{-1}(p_j^n - p_{j-1}^n) + h_j^{-1}\{\{p_3 p(1+\Delta g)^3\}_j^n - \{p_3 p(1+\Delta g)^3\}_{j-1}^n\}] + \xi_{j-1/2}^n p_{j-1/2}^n +$$
$$(p_4)_{j-1/2}^n g_{j-1/2}^n + (p_1)_{j-1/2}^n (fp)_{j-1/2}^n = -M_{j-1/2}^{n-1} + \alpha n[-(ug)_{j-1/2}^{n-1} + (fp)_{j-1/2}^{n-1}] +$$
$$\alpha n[(ug)_{j-1/2}^n - (fp)_{j-1/2}^n - u_{j-1/2}^n g_{j-1/2}^{n-1} + u_{j-1/2}^{n-1} g_{j-1/2}^n\} + p_{j-1/2}^n f_{j-1/2}^{n-1} - p_{j-1/2}^{n-1} f_{j-1/2}^n]$$

$$\Rightarrow \frac{1}{\Pr}[h_j^{-1}(p_j^n - p_{j-1}^n) + h_j^{-1}\{\{p_3 p(1+\Delta g)^3\}_j^n - \{p_3 p(1+\Delta g)^3\}_{j-1}^n\}] + \xi_{j-1/2}^n p_{j-1/2}^n +$$
$$(p_4)_{j-1/2}^n g_{j-1/2}^n + \{(p_1)_{j-1/2}^n + \alpha_n\}(fp)_{j-1/2}^n$$
$$-\alpha_n[\{(ug)_{j-1/2}^n - (ug)_{j-1/2}^{n-1} - u_{j-1/2}^n g_{j-1/2}^{n-1} + u_{j-1/2}^{n-1} g_{j-1/2}^n\} + p_{j-1/2}^n f_{j-1/2}^{n-1} - p_{j-1/2}^{n-1} f_{j-1/2}^n\}]$$
$$= T_{j-1/2}^{n-1}$$

where

$$M_{j-1/2}^{n-1} = \frac{1}{\Pr}[h_j^{-1}(p_j^{n-1} - p_{j-1}^{n-1}) + h_j^{-1}\{\{p_3 p(1+\Delta g)^3\}_j^{n-1} - \{p_3 p(1+\Delta g)^3\}_j^{n-1}\}] -$$
$$[\xi_{j-1/2}^{n-1} p_{j-1/2}^{n-1} + (p_4)_{j-1/2}^{n-1} g_{j-1/2}^{n-1} + (p_1)_{j-1/2}^{n-1}(fp)_{j-1/2}^{n-1}]$$

$$T_{j-1/2}^{n-1} = -M_{j-1/2}^{n-1} + \alpha n[(fp)_{j-1/2}^{n-1} - (ug)_{j-1/2}^{n-1}]$$

The corresponding boundary conditions (7) become

$$f_0^n = 0, \quad u_0^n = 0, \quad g_0^n = 1$$
$$u_j^n = 0, \quad g_j^n = 0$$

If we assume $(f_j^{n-1}, u_j^{n-1}, v_j^{n-1}, g_j^{n-1}, p_j^{n-1})$, $i = 0, 1, 2, 3, \cdots \cdots$, IMAX with initial values equal to those at the proviso x stations. For higher iterates we get

$$\begin{aligned} f_j^{(i+1)} &= f_j^{(i)} + \delta f_j^{(i)} \\ u_j^{(i+1)} &= u_j^{(i)} + \delta u_j^{(i)} \\ v_j^{(i+1)} &= v_j^{(i)} + \delta v_j^{(i)} \\ g_j^{(i+1)} &= g_j^{(i)} + \delta g_j^{(i)} \\ p_j^{(i+1)} &= p_j^{(i)} + \delta p_j^{(i)} \end{aligned} \tag{12}$$

We then insert the right side of the expression (12) in place of f_j^n, u_j^n, v_j^n and g_j^n in Equations (13)-(15) dropping the terms that are quadratic in δf_j^i, δu_j^i, δv_j^i and δp_j^i. This procedure yields the following linear system of algebraic equations:

$$f_j^{(i)} + \delta f_j^{(i)} - f_{j-1}^{(i)} - \delta f_{j-1}^{(i)} = \frac{h_j}{2}\left\{ u_j^{(i)} + \delta u_j^{(i)} + u_{j-1}^{(i)} + \delta u_{j-1}^{(i)} \right\}$$

$$\delta f_j^{(i)} - \delta f_{j-1}^{(i)} - \frac{h_j}{2}\left(\delta u_j^{(i)} + \delta u_{j-1}^{(i)}\right) = (r_1)_j$$

$$\delta u_j^{(i)} - \delta u_{j-1}^{(i)} - \frac{h_j}{2}\left(\delta v_j^{(i)} + \delta v_{j-1}^{(i)}\right) = (r_4)_j$$

$$\delta g_j^{(i)} - \delta g_{j-1}^{(i)} - \frac{h_j}{2}\left(\delta g_j^{(i)} + \delta g_{j-1}^{(i)}\right) = (r_5)_j$$

Momentum equation becomes:

$$\begin{aligned} &h_j^{-1}(v_j^i + \delta v_j^i - v_{j-1}^i - \delta v_{j-1}^i) + \{(p_1)_{j-1/2}^n + \alpha_n\}\{(f\,v)_{j-1/2}^i + \delta(f\,v)_{j-1/2}^i\} \\ &-\{(p_2)_{j-1/2}^n + \alpha_n\}\{(u^2)_{j-1/2}^i + \delta(u^2)_{j-1/2}^i\} + \{g_{j-1/2}^i + \delta g_{j-1/2}^i\} \\ &-(\xi)_{j-1/2}^n\{u_{j-1/2}^i + \delta u_{j-1/2}^i\} + \alpha_n[\{f_{j-1/2}^i + \delta f_{j-1/2}^i\} v_{j-1/2}^{n-1} - \{v_{j-1/2}^i + \delta v_{j-1/2}^i\}] f_{j-1/2}^{n-1}\} \\ &-\left\{\left(p_5\xi^2\right)_{j-1/2}^n + \left(\frac{\delta u_j^i + \delta u_{j-1}^i}{2}\right)\right\} = R_{j-1/2}^{n-1} \end{aligned}$$

$$\begin{aligned} &(s_1)_j \delta v_j^i + (s_2)_j \delta v_{j-1}^i + (s_3)_j \delta f_j^i + (s_4)_j \delta f_{j-1}^i + (s_5)_j \delta u_j^i + (s_6)_j \delta u_{j-1}^i \\ &+(s_7)_j \delta g_j^i + (s_8)_j \delta g_{j-1}^i + (s_9)_j \delta p_j^i + (s_{10})_j \delta p_{j-1}^i = (r_2)_j \end{aligned}$$

Energy equation becomes

$$\frac{1}{\Pr}[h_j^{-1}(p_j^i \div \delta p_j^i - p_{j-1}^i - \delta p_{j-1}^i) + h_j^{-1}\{\{p_3 p(1+\Delta g)^3\}_j^i - \delta\{p_3 p(1+\Delta g)^3\}_j^i\} -$$
$$\{\{p_3 p(1+\Delta g)^3\}_{j-1}^i - \delta\{p_3 p(1+\Delta g)^3\}_{j-1}^i\} - \div \xi_{j-1/2}^n (p_{j-1/2}^i + \delta p_{j-1/2}^i) +$$
$$(p_4)_{j-1/2}^n (g_{j-1/2}^i + \delta g_{j-1/2}^i) + \{(p_1)_{j-1/2}^n + \alpha_n\}\{(f\ p)_{j-1/2}^i + \delta(f\ p)_{j-1/2}^i\}$$
$$- \alpha_n [\{(ug)_{j-1/2}^i + \delta(ug)_{j-1/2}^i\} + (p_{j-1/2}^i + \delta p_{j-1/2}^i) f_{j-1/2}^{n-1}$$
$$- p_{j-1/2}^{n-1}(f_{j-1/2}^i + \delta f_{j-1/2}^i\} - \{(u)_{j-1/2}^i + \delta(u)_{j-1/2}^i\} g_{j-1/2}^{n-1}\}$$
$$\{(g)_{j-1/2}^i + \delta(g)_{j-1/2}^i\} u_{j-1/2}^{n-1}\}] = T_{j-1/2}^{n-1}$$

$$(t_1)_j\, \delta p_j^{(i)} + (t_2)_j\, \delta p_{j-1}^{(i)} + (t_3)_j\, \delta f_j^{(i)} + (t_4)_j\, \delta f_{j-1}^{(i)} + (t_5)_j\, \delta u_j^{(i)}$$
$$\div (t_6)_j\, \delta u_{j-1}^{(i)} + (t_7)_j\, \delta g_j^{(i)} + (t_8)_j\, \delta g_{j-1}^{(i)} = (r_3)_j$$

Where

$$(r_1)_j = f_{j-1}^{(i)} - f_j^{(i)} + h_j u_{j-1/2}^{(i)}$$
$$(r_4)_j = u_{j-1}^{(i)} - u_j^{(i)} \div h_j v_{j-1/2}^{(i)}$$
$$(r_5)_j = g_{j-1}^{(i)} - g_j^{(i)} + h_j p_{j-1/2}^{(i)}$$
$$(r_2)_j = R_{j-1/2}^{n-1} - \left\{ h_j^{-1}(v_j^i - v_{j-1}^i) + \{(p_1)_{j-\frac{1}{2}}^n + \alpha_n\}(fv)_{j-1/2}^i \right\} -$$
$$\{(p_2)_{j-\frac{1}{2}}^n + \alpha_n\}(u^2)_{j-1/2}^{(i)} + g_{j-\frac{1}{2}}^i - \xi_{j-\frac{1}{2}}^n u_{j-\frac{1}{2}}^n + \alpha_n (f_{j-1/2}^i v_{j-1/2}^{n-1} - f_{j-1/2}^{n-1} v_{j-1/2}^i)$$
$$- (p_5 \xi^2)_{j-1/2}^n u_{j-1/2}^i$$

$$(r_2)_j = R_{j-1/2}^{n-1} - \left\{ h_j^{-1}(v_j^i - v_{j-1}^i) + \{(p_1)_{j-\frac{1}{2}}^n + \alpha_n\}(fv)_{j-1/2}^i \right\} -$$
$$\{(p_2)_{j-\frac{1}{2}}^n \div \alpha_n\}(u^2)_{j-1/2}^{(i)} + g_{j-\frac{1}{2}}^i - \xi_{j-\frac{1}{2}}^n u_{j-\frac{1}{2}}^n \div \alpha_n (f_{j-1/2}^i v_{j-1/2}^{n-1} - f_{j-1/2}^{n-1} v_{j-1/2}^i)$$
$$- (p_5 \xi^2)_{j-1/2}^n u_{j-1/2}^i$$
$$(r_3)_j = T_{j-1/2}^{n-1} - \frac{1}{P_r}[h_j^{-1}(p_j^{(i)} - p_{j-1}^{(i)}) + h_j^{-1}(p_3 p(1+\Delta g)^3\}_j^i - \{\{p_3 p(1 \div \Delta g)^3\}_{j-1}^i] +$$
$$\xi_{j-1/2}^n p_{j-1/2}^i + (p_4)_{j-1/2}^n g_{j-1/2}^i + \{(p_1)_{j-1/2}^n + \alpha_n\}(f\ p)_{j-1/2}^i -$$
$$\alpha_n [\{(ug)_{j-1/2}^i + p_{j-1/2}^i f_{j-1/2}^{n-1} - p_{j-1/2}^{n-1} f_{j-1/2}^i - (u)_{j-1/2}^i g_{j-1/2}^{n-1}\}(g)_{j-1/2}^i u_{j-1/2}^{n-1}\}]$$

Thus the coefficients of momentum equation are

$$(s_1)_j = h_j^{-1} + \frac{1}{2}\left\{(p_1)^n_{j-\frac{1}{2}} + \alpha_n\right\} f_j^{(i)} - \frac{\alpha_n}{2} f_{j-1/2}^{n-1} + \frac{1}{2}\xi^n_{j-\frac{1}{2}}$$

$$(s_2)_j = -h_j^{-1} + \frac{1}{2}\left\{(p_1)^n_{j-\frac{1}{2}} + \alpha_n\right\} f_{j-1}^{(i)} - \frac{\alpha_n}{2} f_{j-1/2}^{n-1} + \frac{1}{2}\xi^n_{j-\frac{1}{2}}$$

$$(s_3)_j = \frac{1}{2}\left\{(p_1)^n_{j-\frac{1}{2}} + \alpha_n\right\} v_j^{(i)} - \frac{\alpha_n}{2} v_{j-1/2}^{n-1}$$

$$(s_4)_j = \frac{1}{2}\left\{(p_1)^n_{j-\frac{1}{2}} + \alpha_n\right\} v_j^{(i)} - \frac{\alpha_n}{2} v_{j-1/2}^{n-1}$$

$$(s_5)_j = -\frac{1}{2}\{(p_2)^n_{j-\frac{1}{2}} + \alpha_n\} u_{j-1}^{(i)} - \frac{1}{2}(p_5\xi^2)^n_{j-\frac{1}{2}}$$

$$(s_6)_j = -\frac{1}{2}\{(p_2)^n_{j-\frac{1}{2}} + \alpha_n\} u_{j-1}^{(i)} - \frac{1}{2}(p_5\xi^2)^n_{j-\frac{1}{2}}$$

$$(s_7)_j = \frac{1}{2}$$

$$(s_8)_j = \frac{1}{2} \qquad (13)$$

$$(s_9)_j = 0$$

$$(s_{10})_j = 0$$

Again the coefficients of energy equation are

$$(t_1)_j = \frac{1}{P_r}[h_j^{-1} + p_3 h_j^{-1}\{(1+\Delta g)^3\}'_j] + \frac{1}{2}\xi^n_{j-1/2} + \frac{1}{2}\{(p_1)'_{j-1/2} + \alpha_n\} f'_j - \frac{\alpha_n}{2} f^{n-1}_{j-1/2}$$

$$(t_2)_j = \frac{1}{P_r}[-h_j^{-1} - p_3 h_j^{-1}\{(1+\Delta g)^3\}'_{j-1}] + \frac{1}{2}\xi^n_{j-1/2} + \frac{1}{2}\{(p_1)'_{j-1/2} + \alpha_n\} f'_{j-1} - \frac{\alpha_n}{2} f^{n-1}_{j-1/2}$$

$$(t_3)_j = \frac{1}{2}\{(p_1)^n_{j-1/2} + \alpha_n\} p'_j + \frac{\alpha_n}{2} p^n_{j-1/2}$$

$$(t_4)_j = \frac{1}{2}\{(p_1)^n_{j-1/2} + \alpha_n\} p'_{j-1} - \frac{\alpha_n}{2} p^{n-1}_{j-1/2}$$

$$(t_5)_j = -\frac{\alpha_n}{2} g'_j - \frac{1}{2} g^{n-1}_{j-1/2}$$

$$(t_6)_j = -\frac{\alpha_n}{2} g'_{j-1} - \frac{1}{2} g^{n-1}_{j-1/2} \qquad (14)$$

$$(t_7)_j = \frac{1}{P_r}[3 h_j^{-1} p_3 p'_j \Delta\{(1+\Delta g)^2\}'_{j-1}] + \frac{1}{2}\{(p_4)'_{j-1/2} - \alpha_n[\frac{1}{2}u'_j + \frac{1}{2}u^{n-1}_{j-1/2}]$$

$$(t_8)_j = \frac{1}{P_r}[-3 h_j^{-1} p_3 p'_{j-1} \Delta\{(1+\Delta g)^2\}'_{j-1}] + \frac{1}{2}\{(p_4)'_{j-1/2} - \alpha_n[\frac{1}{2}u'_j + \frac{1}{2}u^{n-1}_{j-1/2}]$$

$$(t_9)_j = 0$$

$$(t_{10})_j = 0$$

The boundary condition (13) becomes

$$\partial f_0 = 0 \ , \ \partial u_0 = 0, \partial \theta_0 = 1$$
$$\partial u_j = 0, \partial \theta_j = 0 \qquad (15)$$

which just express the requirement for the boundary conditions to remain during the iteration process. Now the system of linear Equations (13) and (14) together with the boundary conditions (15) can be written in matrix or vector form, where the coefficient matrix has a block tri-diagonal structure. The whole procedure, namely reduction to first order followed by central difference approximations, Newton's quasi-linearization method and the block Thomas algorithm, is well known as the Keller- box method